EndoAnchors in abdominal aortic endografts: *in-vitro* and clinical outcome

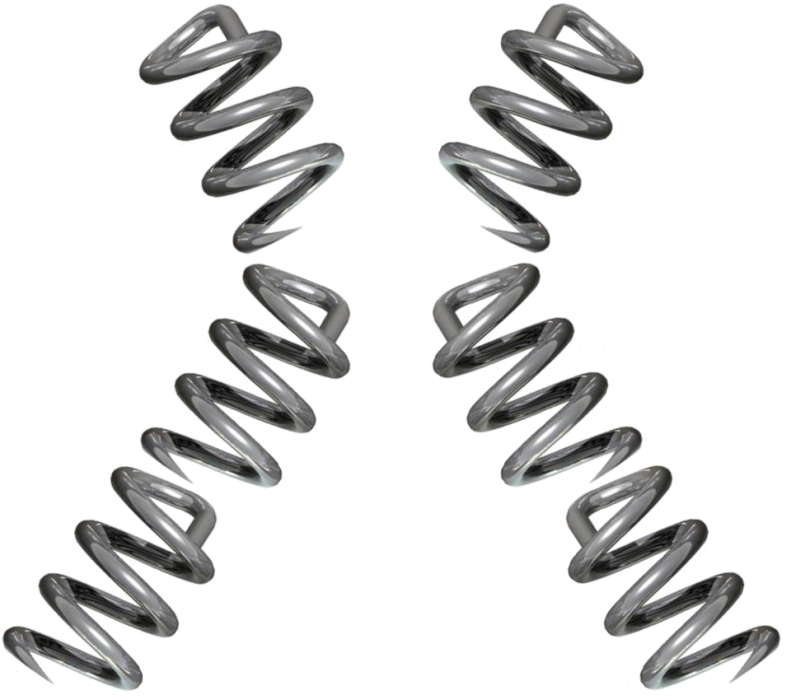

Master Thesis Technical Medicine

"EndoAnchors in abdominal aortic endografts: *in-vitro* and clinical outcome"

Master thesis of:
J.J.M. Vermeulen[1,2]

Supervisors/graduation board members:

Medical supervisor	Dr. J.P.P.M. de Vries[1]
Technical supervisor	Prof. Dr. Ir. C.H. Slump[3]
Process supervisor	Drs. R.J. Haarman[2]
Technical supervisor	S.R. Goudeketting MSc.[1,2]

External graduation board member:
Dr. E. Groot Jebbink[4,5]

Graduation date:
13-07-2018

Affiliations:
[1] Department of Vascular Surgery, St. Antonius Hospital, Nieuwegein, The Netherlands
[2] Technical Medicine, Faculty of Science and Technology, University of Twente, Enschede, The Netherlands
[3] MIRA Institute of Biomedical Technology and Technical Medicine, University of Twente, Enschede, The Netherlands
[4] Multi-Modality Medical Imaging, Faculty of Science and Technology, University of Twente, Enschede, The Netherlands
[5] Physics of Fluids, Faculty of Science and Technology, University of Twente, Enschede, The Netherlands

Summary

The main challenge of an endovascular aneurysm repair (EVAR) procedure to treat an abdominal aortic aneurysm (AAA) is fixation of the endograft in the aortic neck. Inaccurate fixation can cause complications, such as type IA endoleak, endograft migration, thrombosis, risk of rupture and need for reintervention. The Heli-FX EndoAnchor system (Medtronic Vascular, Santa Rosa, CA, USA) ensures endograft fixation and seal in the infrarenal aortic neck by penetrating both the endograft's fabric and the aortic wall during EVAR. Despite the good outcomes of EndoAnchor usage, endoleaks are detected in 22.2% of the patients during follow-up. Furthermore, penetration and configuration of the EndoAnchors may influence the clinical outcome. Therefore, the aim of this thesis was to investigate the effect of the positioning and penetration depth of EndoAnchors with the focus on proximal fixation on the occurrence of endoleaks and migration.

A clinical study on the sustainability of individual EndoAnchors was performed. Measurements were performed on CT data of patients which were treated therapeutically with EndoAnchors for type IA endoleaks. Afterwards, clinical information on applied EndoAnchor configurations was used to create a measurement protocol and an *in-vitro* measurement setup was developed. This setup was used to provide a validated environment to test the effect of the configuration of EndoAnchor deployment on the sensitivity of endograft migration.

The follow-up study demonstrated that 97.4% of the initially good implanted EndoAnchors remained good at a median follow-up of 13 months. The *in-vitro* study showed that the endograft remained sensitive to migration, when there is no circumferential EndoAnchor deployment. The distance between EndoAnchors and EndoAnchor deployment below each other demonstrated to favourably influence the migration resistance.

Overall, positioning and penetrating of EndoAnchors demonstrated to have an important effect on the occurrence of migration and the durability of individual EndoAnchors. Good deployed EndoAnchors have an excellent sustainability over time. Furthermore, EndoAnchors generate larger migration resistance when deployed circumferential or close to or below each other. Future research should focus on the effect of EndoAnchors on migration behaviour in different endografts and environments which mimic challenging aortic necks.

List of abbreviations

AAA	Abdominal aortic aneurysm
ANCHOR	Aneurysm treatment using the Heli-FX aortic securement system global registry
CLL	Centre lumen line
CT	Computed tomography
CTA	Computed tomography angiography
EMF	Endograft migration force
EVAR	Endovascular aneurysm repair
IFU	Instructions for use
IQR	Interquartile range
mm	Millimetres
MPa	Mega pascal
N	Newton

Table of Contents

1. General introduction

1.1 Abdominal aortic aneurysms and EndoAnchors

Abdominal aortic aneurysm (AAA) is a frequent occurring disease, which has a prevalence of 1% among men and women above the age of 65 years.[1] An aneurysm is defined as a permanent enlargement of the aortic diameter larger than 3 cm or at least 1.5 times its normal aortic diameter.[2] An AAA occurs due to a weakness in the media and/or adventitia wall of the abdominal aorta. This is characterized by destruction of elastin, collagen and smooth muscle cells, which results in thinning of the medial and/or adventitia wall.[3] It can best be described as "a chronic inflammatory condition with an accompanying proteolytic imbalance".[4] Risk factors are male sex, high age, smoking, diabetes mellitus, hypertension, atherosclerosis, a high level of cholesterol, and familial AAA.[5] When an AAA exceeds a diameter of 5.5 cm for men and 5.0 cm for women or grows more than 1 cm per year, the rupture risk increases. Rupture of an AAA has a high mortality rate (80%). Therefore, early detection and follow-up of AAA is necessary to perform early repair of the aneurysm.[1,6] However, most AAA's are asymptomatic and are only detected as an incidental finding.[6,7]

Elective surgery is performed to treat an AAA when the risk of rupture is higher than the operative risks. The risk of rupture, anticipated quality of life after operation and the risk of surgical treatment will be defined for each individual patient to determine the type of surgical treatment. Open surgical repair is considered as the golden standard, but it has a mortality rate varying between 4% and 8.4% depending on the surgeon's experience and the patient's cardiovascular condition. Since 1990, endovascular aneurysm repair (EVAR) is an alternative treatment for AAA. EVAR reduces the surgical risk because of the minimally invasive technique, resulting in less blood loss, shorter recovery time, and reduced hospital stay. The technique involves implantation of an endograft into the vessel lumen to exclude the aneurysm. The typical design of an endograft consists of a main trunk for the proximal aorta and two branches for the iliac arteries. This is divided in two or three separate components. One component includes the main aortic trunk and one branch for an iliac artery. This component also has an opening for attachment of the second component, which will be deployed in the contralateral iliac artery. A third component can be used as an extension of one of the branches into the iliac artery for more accurate positioning. Figure 1 shows the initial endograft placement.[2,6,7]

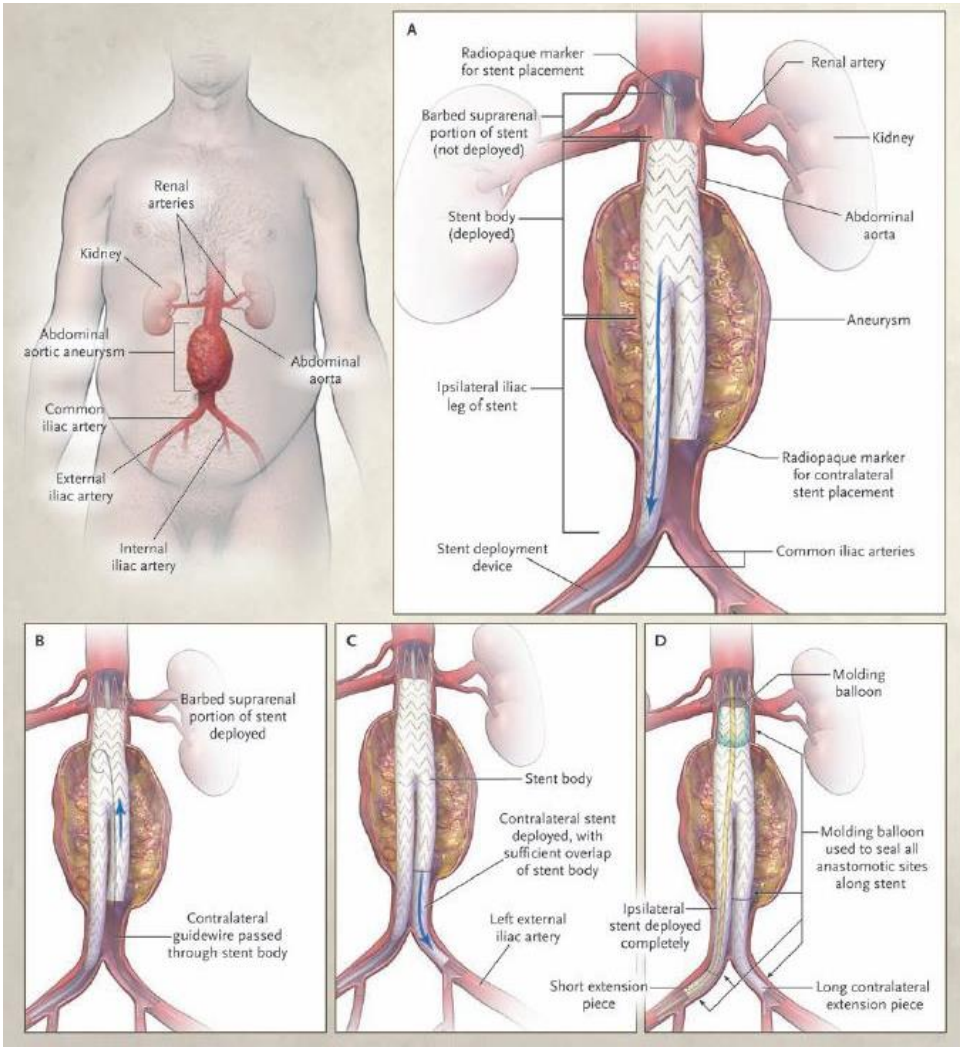

Figure 1. Endograft placement during an EVAR procedure[6]

Besides the benefits of the EVAR procedure, there are also some complications which can occur, such as endoleaks, graft migration, thrombosis, risk of rupture and need for re-intervention[7–9]. An endoleak is described as blood flow outside the endograft, but within the aneurysm sac. This can occur along every part of the endograft, which can be a result of inaccurate sealing or fixation, or from retrograde flow into the aneurysm sac. According to the Society for Vascular Surgery, migration is defined as movement of the endograft larger than ten millimetres or any movement of the endograft leading to symptoms or requiring therapy[8,10].

The main challenge of an EVAR procedure is fixation of the endograft in the aortic neck. The current fixation of endografts is achieved by oversizing the proximal diameter of the endograft compared to the aortic neck diameter. Usually an endograft is chosen with a diameter 10% to 20% larger than the diameter of the aortic neck. This amount of oversizing results in a reduced type IA endoleak rate, which is defined as a gap between the graft and the vessel wall at the proximal sealing zone[11–13]. Incomplete dilatation, inaccurate sizing of the endograft and short, angulated aortic necks can cause type IA endoleaks[11].

Besides this oversizing, migration and endoleaks can also be prevented with hooks and barbs. However, these fixation and sealing techniques are not always successful. Another alternative to prevent or overcome these complications is the use of EndoAnchors. The Heli-FX EndoAnchor System (Medtronic Vascular, Santa Rosa, CA, USA) creates a fixation between the endograft and the aortic wall. This fixation is comparable to the integrity of a surgical hand-sewn anastomosis. In this way, dynamic migration forces on the proximal endograft can be overcome. It can also be used for primary sealing in challenging necks. Especially short, angulated necks and necks with large diameters are challenging to fixate with solely an endograft[11–13].

The Heli-FX EndoAnchor System consists of two complementary devices: a guide and an applier. Both components are disposable and designed to implant one EndoAnchor at a time at the proper location. Each EndoAnchor has a helical shape with a diameter of 3 mm and length of 4.5 mm. It is designed to penetrate the aortic wall atraumatically with a maximum of approximately 0.5 to 1 mm outside the aortic wall (Figure 2). Furthermore, the design ensures a safety mechanism that the EndoAnchor cannot pass through the graft fabric. The implantation of EndoAnchors is performed in two stages; first, the EndoAnchor is deployed halfway with one winding and then, the EndoAnchor is fully deployed. In this way, it is possible to retract the EndoAnchor at the halfway point and reposition the EndoAnchor in case of suboptimal deployment.[14]

Figure 2. The design of the EndoAnchor, which is manufactured from medical wire 0.5 mm in diameter [14]

EndoAnchors are a relatively new technique used in EVAR procedures. It is necessary to understand the technical properties, such as fixation, design, and durability of this device. Knowledge about the forces acting upon the device in situ can help to understand the requirements of this device. Liffman et al.[15] performed such an analysis for several endografts, used during an EVAR procedure. They used a simplified model, which assumed nonpulsatile, turbulent flow in a rigid, symmetrical graft. The study showed that lateral forces are larger in curved vessels than in a straight vessel. This could result in displacement from both proximal and distal ends, depending on the graft fixation in each landing zone. Infrarenal grafts are more likely to be displaced according to the models of Liffman et al.[15] This displacement tends to occur at the proximal site. Overall, Liffman et al.[15] showed that the forces on the graft were more affected by size rather than the curvature of the graft. The study does not include EndoAnchors. However, the results about the effect of forces on the endograft may be comparable to forces that EndoAnchors endure after implantation, since they penetrate the endograft and aortic wall.

Patients with loss of proximal seal of the endograft have significantly more dilated aortic necks than patients without this loss. Literature implies that neck dilation occurs faster after EVAR than open repair within two years.[16] However, long-term results show no significant differences between dilatation rates at infrarenal and suprarenal levels between EVAR and open surgical repair.[17,18] This could indicate that outward radial forces of the endografts do not have a big influence on the aneurysm neck, but it may occur more by natural progression of the disease. EndoAnchors have shown to have a protective effect on and significant reduction of aortic neck dilatation, which could be caused by a counteracting force of the EndoAnchors on the aortic wall.[18,19]

The main use of EndoAnchors is to provide proximal fixation of the endograft to the aortic neck. The study of Melas et al.[20] demonstrated that the use of EndoAnchors significantly improves this proximal fixation. Force was applied on a endograft with penetrated EndoAnchors and most times the endograft was pulled out or the aorta ruptured. The mean displacement force (i.e. 20 mm displacement) applied to endografts with no active fixation was 8.29 ± 1.15 N[20], whereas the natural drag force of the blood is calculated as approximately 5 N.[21] The application of EndoAnchors increased the level of fixation to a conventional hand-sewn vascular anastomosis with no differences between endografts with and without hooks and barbs.[20] These results are very promising. Furthermore,

Goudeketting et al.[22] demonstrated the importance of good EndoAnchor penetration with the aortic wall to achieve proper fixation, which can prevent endoleak occurrence. Patients with endoleaks had more "borderline" or "non-penetrating" EndoAnchors than patients without endoleaks. Furthermore, EndoAnchors deployed at the location of the endoleak more frequently had borderline or no penetration. This implies that the location where EndoAnchors are placed can influence the penetration success rate.[22]

Several studies report the good outcomes after EndoAnchor use. Proximal fixation is improved and less endoleaks and migration occur. Jordan et al.[23] showed a rate of 98.1% for technical successful implantation of EndoAnchors, meaning that the deployment was satisfactory and no fracture or loss of integrity occurred. However, endoleaks were detected in 22.2% of the patients during follow-up.[23] Literature is inconclusive about the cause of endoleaks after EndoAnchor deployment. Thrombus and undersizing could be a cause of these complications.[11,23–25] However, penetration and configuration of the EndoAnchors can also influence their clinical outcome.[22] The aim of the research reported in this thesis is to investigate the effect of the positioning and penetration depth of EndoAnchors with the focus on proximal fixation on the occurrence of endoleaks and migration.

1.2 Outline thesis

This thesis is focused on the use of EndoAnchors in abdominal aortic endografts and the effect of them on the occurrence of complications like endoleaks and migration. Therefore, the objective can be described as: "EndoAnchors in abdominal aortic endografts: *in-vitro* and clinical outcome".

The first chapter of this thesis has given an introduction about AAA and the use of EndoAnchors, where the goal of this thesis is described.

The second chapter is a study on the clinical sustainability of EndoAnchors. A follow-up study is executed, where measurements on CT data of patients are performed. The outcome of these measurements is compared to clinical information of these patients to determine the durability of EndoAnchors over time.

The third chapter describes the development and validation of a measurement setup to perform an *in-vitro* study on EndoAnchors. The goal is to determine which kind of measurement setup can provide a validated environment to test the effect of the positioning and penetration depth of EndoAnchors on endograft migration with pulling force in silicon models.

The fourth chapter contains an *in-vitro* study to determine the effect of the configuration of EndoAnchors deployment on the sensitivity of endograft migration. This study is performed with the measurement setup, which is described in chapter three.

The fifth chapter summarizes and discusses the main findings of the thesis regarding the effect of the positioning and penetration depth of EndoAnchors in abdominal aortic endograft. This is focused on the proximal fixation and the occurrence of endoleaks and migration. Future perspectives regarding research about EndoAnchors are also discussed.

2. Sustainability of individual EndoAnchor implants in therapeutic use during endovascular aortic aneurysm repair.

Kim van Noort, MSc[1,2], Jenske J.M. Vermeulen, BSc[1,2], Seline R. Goudeketting, MSc [1,2], Kenneth Ouriel, MD[3], William D. Jordan Jr, MD[4], Jean M. Panneton, MD[5], Cornelis H. Slump, MSc, PhD[2], Jean-Paul P.M. de Vries, MD, PhD[6]

Submitted: Journal of Vascular Surgery, June 20th, 2018

Affiliations:
[1] Department of Vascular Surgery, St. Antonius Hospital, Nieuwegein, The Netherlands
[2] MIRA Institute of Biomedical Technology and Technical Medicine, University of Twente, Enschede, The Netherlands
[3] Syntactx, New York City, New York, USA
[4] Department of Vascular Surgery, Emory University School of Medicine, Atlanta, GA, USA
[5] Division of Vascular Surgery, Eastern Virginia Medical School, Norfolk, VA, USA
[6] Devision of Surgery, Department of Vascular Surgery, University Medical Centre Groningen, Groningen, The Netherlands

Declaration of conflict of interests

JMP, WDJ and JPdV are consultants and on the Scientific Advisory Board for Medtronic, Inc.

This research received a restricted grant from Medtronic, Inc.

2.1 Abstract

Introduction: The aim of this study was to investigate changes of individual EndoAnchor implant penetration depths and angles on sequential computed tomography angiography (CTA) scans after therapeutic use in endovascular aortic aneurysm repair.

Methods: Patients were selected from the Aneurysm Treatment Using the Heli-FX Aortic Securement System Global Registry (ANCHOR;NCT01534819). Inclusion criteria were indication for use of EndoAnchor implants to therapeutically treat a type IA endoleak, and at least two available postoperative contrast-enhanced CTAs. Exclusion criteria were the use of adjunct procedures like proximal extension cuffs and giant stents. Penetration depth of each EndoAnchor implant was determined as (1) good penetration, when the EndoAnchor implant penetrates ≥ 2 mm into the aortic wall, (2) borderline penetration, when the EndoAnchor implant penetrates < 2 mm into the aortic wall or when there is a gap between the endograft and the aortic wall or (3), no penetration, when the EndoAnchor implant does not penetrate the aortic wall at all. The orthogonal and the longitudinal angles of every EndoAnchor implant with the aortic wall were determined. The penetration depth and angles of all EndoAnchor implants which had a good penetration on the first postprocedural CTA scan were investigated on the last available postprocedural CTA scan.

Results: A total of 54 patients were included in this study and a total of 360 EndoAnchor implants were deployed (median of 6 [interquartile range (IQR), 4-9] EndoAnchor implants per patient). Thirty-five patients had no type IA endoleak on both the first and last postprocedural CTA scan. Eighteen patients had a type IA endoleak on the first postprocedural CTA scan of which 4 resolved over time. Median[IQR] follow-up was 13 [8-23] months. No new type IA endoleak occurred during follow-up. On the first postprocedural CTA scan respectively 187 (51.9%), 69 (19.2%) and 104 (28.9%) EndoAnchor implants had good, borderline and no penetration respectively. Of the initial 187 good penetrating EndoAnchor implants 182 remained good (97.4%), 4 became borderline penetrating (2.1%) and one became non-penetrating (0.5%). The median[IQR] orthogonal angles of the good penetrating EndoAnchor implants on the first postprocedural CTA-scan, and the last follow-up CTA scan were 92 [85-98] degrees and 90 [84-97] degrees respectively (P=0.822). For the longitudinal angles, a median [IQR] of 85 [71-96] degrees and 84 [70-96] degrees were found at the first and last postprocedural CTA scan (P=0.043).

Conclusions: Sustainability of individual EndoAnchor implants is excellent. A total of 97.4% of the good penetrating EndoAnchor implants remained good at a median follow-up of 13 months. Only five EndoAnchor implants became borderline or non-penetrating without any clinical consequence.

2.2 Introduction

The Helix-FX EndoAnchor System (Medtronic Vascular, Santa Rosa, CA, USA) is designed to penetrate both the endograft's fabric and aortic wall to ensure endograft fixation and seal in the infrarenal aortic neck during endovascular aortic aneurysm repair (EVAR). EndoAnchor implants can be used to treat acute and late type IA endoleaks in therapeutic setting, while they can prevent migration when used prophylacticly.[12,14,25,26] When deployed circumferentially a surgical hand-sewn anastomosis is approximated, if the EndoAnchor implants are successfully deployed.[20,27]

Recent publications showed aortic neck diameter and neck calcium thickness as independent predictors for individual EndoAnchor implant failure.[22] Moreover, an analysis was performed on the penetration depth and angle of each EndoAnchor implant.[28] These studies showed that a greater number of non-penetrating EndoAnchor implants was associated with an increased risk for type IA endoleaks, and 30% of EndoAnchor implants were deployed beyond the recommended use. (i.e. were positioned above the fabric, within thrombus or below the aortic neck). Besides deployment beyond the recommended use, technical positioning failure may cause the EndoAnchor implant not to penetrate the aortic wall perpendicularly and therefore not completely penetrate the aortic wall.

These factors may also be important for the sustainability of the EndoAnchor implants in the aortic wall over time. The aim of this study was to investigate changes of individual EndoAnchor implant penetration depths and angles over time and potential clinical sequelae.

2.3 Method

2.3.1 Patient selection

Patients were selected from the dataset of the Aneurysm Treatment Using the Heli-FX Aortic Securement System Global Registry (ANCHOR; NCT01534819). Inclusion criteria for selection of the current study population were indication for use of EndoAnchor implants to therapeutically treat type IA endoleak and at least two

sequential postoperative contrast-enhanced computed tomography angiographies (CTA) of sufficient quality after primary EndoAnchor implant. Patients with CTA scans with glue or metal artefacts were excluded, as were CTAs with slice thickness > 3 mm. Patients with aortic cuffs were excluded from the data set, because EndoAnchor implants are not designed to penetrate 2 or more graft components. Moreover, a resolved endoleak might not only be a result of EndoAnchor implant placement, it may also be due to the aortic cuff.

A larger cohort (n=86) was previously used to describe penetration depth and angles of EndoAnchor implants on the first postprocedural CTA scans.[28] Thirty-two of these 86 patients did not have a second postprocedural CTA scan and were excluded in the current study.

2.3.2 Imaging studies and measurement protocol

Measurements were performed on the first postprocedural (implant of EndoAnchors) CTA scan and on the last available follow-up CTA scan (i.e. the last available or the last one before eventual reintervention) on a 3Mensio vascular workstation V9.0 SP1 (Pie Medical Imaging BV, Maastricht, The Netherlands). This study cohort and measurement protocol were previously used to assess the penetration depth and angles of EndoAnchor implants on the first postprocedural CTA scan.[28] A centre lumen line (CLL) was semi-automatically drawn through the lumen of the aorta and adjusted manually if needed. Location of the orifices of the renal arteries, EndoAnchor implants, proximal endograft fabric markers and aortic bifurcation were identified.

Anatomical characteristics

Core lab analysis (Syntactx, New York, NY) was performed for the anatomical characteristics on the first and last postprocedural CTA scan. Anatomical characteristics consisted of; suprarenal aortic diameter, aortic diameter at the level of the lowest renal artery, proximal neck length (with distal boundary where there is a 10% increase of the diameter at the level of the lowest renal artery), visual neck length, neck tortuosity index, maximum aneurysm sac diameter, suprarenal angulation, infrarenal angulation, neck thrombus thickness and circumference, and neck calcification thickness and circumference.

Clinical outcome

The clinical outcome between the sequential CTA scans was investigated. There were three possibilities; 1) No change, which means a type IA endoleak or none on both follow-up moments, 2) Occurrence of type IA endoleak between the follow-up moments or, 3) Resolution of a type IA endoleak after the first postprocedural CTA scan.

EndoAnchor implant penetration analysis

EndoAnchor implant penetration was determined as (1) good penetration, when the EndoAnchor implant penetrates the endograft as well as ≥ 2 mm into the aortic wall, (2) borderline penetration, when the EndoAnchor implant penetrates the endograft, but < 2 mm into the aortic wall or when there is a gap between the endograft and the aortic wall (3), no penetration, when the EndoAnchor implant does not penetrate the aortic wall at all. Differences between EndoAnchor implant penetration over time were analysed.

Only EndoAnchor implants with good penetration on the first postprocedural CTA scan were analysed on the last postprocedural CT scan. Previous study showed that borderline penetrating EndoAnchor implants are comparable in clinical outcome to non-penetrating EndoAnchor impants.[22] Both borderline and non-penetrating EndoAnchor implants will not lead to an increased seal between endograft and aortic wall and will never become good penetrating. The measurements were performed independently by two experienced observers (KN, JV). A third observer opinion (JPdV) was requested if the outcome was inconclusive.

EndoAnchor implant angle analysis

The orthogonal and longitudinal penetration angles were measured according to the validated method previously described in the study of Goudeketting et al.[28] The technical background can be found in appendix A. Differences between the orthogonal and longitudinal angles over time were analysed.

2.3.3 Statistical analysis

Statistical analyses were performed with SPSS version 24 (IBM Corp, Armonk, NY, USA). Normality of data was tested with the Shapiro-Wilk test. Normality of data could not be assumed. Therefore, data was represented as median [IQR].

Differences between variables were tested with the Mann-Whitney U test. P-values were considered significant when two-tailed $\alpha < 0.05$.

2.4 Results

A total of 54 patients of the 86 patients described in a previous study[28] were included in the current analysis, and a total of 360 EndoAnchor implants were deployed (median of 6 [interquartile range (IQR), 4-9] EndoAnchor implants per patient). Median time between the EVAR procedure with EndoAnchor implants and the first postprocedural CTA scan was 34 days [IQR, 24- 43 days], and 13 months [IQR, 8-23 months] for the last available post EndoAnchor implant CTA scan.

Anatomical characteristics

Table 1 shows the anatomical characteristics on the first and the last postprocedural CTA scans. Maximum sac diameter became significantly smaller during follow-up (P<0.001). Other anatomical characteristics remained unchanged.

Clinical outcome

Thirty-six patients had no type IA endoleak on both the first and last postprocedural CT scan. Eighteen patients had a type IA endoleak on the first postprocedural CT scan of which six resolved over time (without additional treatment). One persistent type IA endoleak was treated with coiling of the AAA 6 months after placement of the EndoAnchor implants. In one patient, the type IA endoleak was resolved after deployment of additional EndoAnchor implants 23.5 months after the initial procedure. In one patients, ten EndoAnchor implants were deployed at 12.7 months after the initial procedure, however, without success. A conversion to open repair was performed at 25.6 months. In one patient, an aortic extender cuff with additional EndoAnchor implants were deployed at 2.1 months after the initial procedure. In fourteen patients, no reinterventions were performed to resolve the persistent type IA endoleak.

EndoAnchor implant penetration analysis

On the first postprocedural CTA scan respectively 187 (51.9%), 69 (19.2%) and 104 (28.9%) EndoAnchor implants had good, borderline and no penetration. The two observers were inconclusive in 38 EndoAnchor implants (20.3%) and consensus was found with the third observer. Only the good penetrating EndoAnchor implants were measured on the last postprocedural CTA scan. A total

of 182 EndoAnchor implants remained good penetrating after follow-up (97.4%), four became borderline penetrating (2.1%) and one became non-penetrating (0.5%).

Figure 3 shows an example of a stable configuration of two EndoAnchor implants on sequential CTA scans. A total of six EndoAnchor implants were deployed in this patient, all remained in a good position over time.

Five EndoAnchor implants (2.6%) in four patients had a change in configuration over time, all without any clinical sequelae. Figure 4 and Table 2 show a patient where one EndoAnchor implant became borderline and one became non-penetrating. In this case, only four EndoAnchor implants were initially deployed in the aortic neck, instead of the recommended use of at least six. On both CTA scans, a type IA endoleak was visible. The neck has a conical shape and is only 3.2 mm in length, which is beyond the recommended use for standard EVAR with EndoAnchor implants. During follow-up, dilatation of the aortic neck occurred, creating a growing gap of malapposition between the aortic wall and endograft. Therefore, the EndoAnchor implants became borderline and non-penetrating, respectively.

Figure 5 and Table 3 show another patient with a change in penetration depth of one EndoAnchor implant after 34 months of follow-up. Interestingly, only two EndoAnchor implants were good penetrating at the first postprocedural CT scan of which one became borderline penetrating. The endograft was initially deployed low, and there was a type IA endoleak visible on both CTA scans. This challenging neck had a large calcium load at the location of the type IA endoleak, consequently no EndoAnchor implants were penetrating the aortic wall. Moreover, there was a gap between the aortic wall and endograft, which could not be resolved with EndoAnchor implants. It is obvious most of the EndoAnchor implants in this patient have been used beyond the recommended use. The EndoAnchor implant became borderline because the aneurysm sac extended cranially creating a gap between the fabric and aortic wall at the location of the EndoAnchor implant, and thus per definition this implant became borderline penetrating. Dilatation of the aortic neck may not be stopped by just one good penetrating EndoAnchor implant.

Table 1: Anatomical characteristics on the first and last postprocedural CT scan

Anatomical characteristics	**First CTA**	**Last CTA**	**P-value**
Suprarenal aortic diameter, mm	26.2 [24.7 - 27.5]	25.7 [24.8 - 27.6]	0.228
Aortic diameter at lowest renal, mm	25.5 [23.6 - 27.8]	25.4 [23.9 - 27.3]	0.472
Proximal neck length, mm	10.4 [6.5 - 20.9]	11.0 [5.6 - 19.6]	0.820
Maximum sac diameter, mm	59.3 [52.6 - 69.1]	56.0 [49.0 - 66.4]	<0.001[a]
Suprarenal angulation, °	13.0 [7.8 - 19.5]	13.0 [8.0 - 17.3]	0.102
Infrarenal angulation, °	15.5 [7.8 - 25.0]	14.0 [8.0 - 21.3]	0.268
Neck thrombus average thickness, mm	0.0 [0.0 - 0.0]	0.0 [0.0 - 0.0]	0.514
Neck thrombus circumference, mm	0.0 [0.0 - 0.0]	0.0 [0.0 - 0.0]	0.594
Neck calcium average thickness, mm	0.0 [0.0 - 0.0]	0.0 [0.0 - 0.0]	0.833
Neck calcium circumference, mm	0.0 [0.0 - 0.0]	0.0 [0.0 - 0.0]	0.528

Data represented as median [interquartile range (Q1-Q3)]. [a] Values were significantly different with $\alpha < 0.05$.

The remaining two EndoAnchor implants became borderline at 13 months and 38 months follow-up. In one patient, ten EndoAnchor implants were positioned of which three had a good position, one a borderline penetration and six no penetration on the first postprocedural CTA scan. There was no type IA endoleak visible on both follow-up moments and no change in anatomical characteristics was observed. The changing EndoAnchor implant was positioned in an area with a high calcium load.

In the other patient, also ten EndoAnchor implants were deployed (five with good deployment, one borderline penetration and four non- penetrating EndoAnchor implants on the first postprocedural CTA scan). There was a type IA endoleak visible on the first postprocedural CTA scan however, it resolved after 38 months of follow-up. At the location of the changing EndoAnchor implant there was a slight increase in aortic diameter (2 mm), causing the EndoAnchor implant to become borderline penetrating.

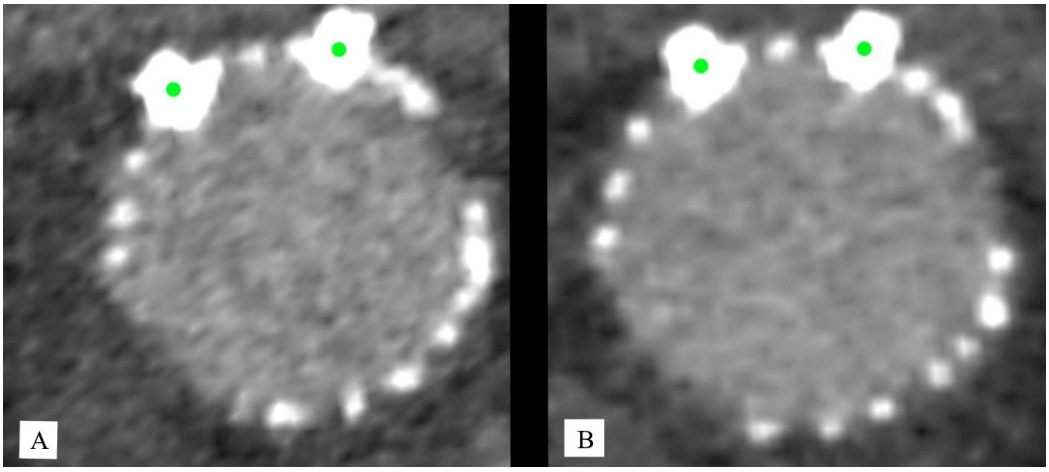

Figure 3. An example of stable EndoAnchor implants. A) One-month postprocedural CTA scan. A total of 6 EndoAnchor implants were positioned in this patient. At this axial slice, only two EndoAnchor implants (green dots) are visible, both are penetrating the aortic wall. The other four EndoAnchor implants (not visible) are also penetrating the aortic wall. B) Postprocedural CTA scan (13 months). All EndoAnchor implants remain unchanged (green dots + four EndoAnchor implants which are not visible on this image).

Table 2. Characteristics of the aorta, endograft and EndoAnchor implants where one EndoAnchor implant became borderline penetrating and one non-penetrating (Figure 4).

Characteristics		
Follow-up, months	11	
Endograft	Cook Zenith	
Size endograft, mm	32	
Oversizing, % (at baseline)	23.4%	
Number of EndoAnchor Implants	4	
	30 days CT scan	*11 months CT scan*
Good penetration, N	2	0
Borderline penetration, N	0	1
No penetration, N	2	3
Endoleak	Yes	Yes
Measurements		
Suprarenal aortic diameter, mm	26.3	25.2
Aortic diameter at lowest renal, mm	24.5	27
Aortic diameter 5-mm below lowest renal, mm	28.3	32.1
Aortic diameter 10-mm below lowest renal, mm	30.9	35.2
Proximal neck length, mm	3.2	2.6
Maximum sac diameter, mm	51.5	48.5
Suprarenal angulation, °	10	5
Infrarenal angulation, °	9	6
Infrarenal angulation to bifurcation, °	16	29
Neck thrombus average thickness, mm	0	1.5
Neck thrombus circumference, °	0	29
Neck calcium average thickness, mm	0	0
Neck calcium circumference, °	0	0

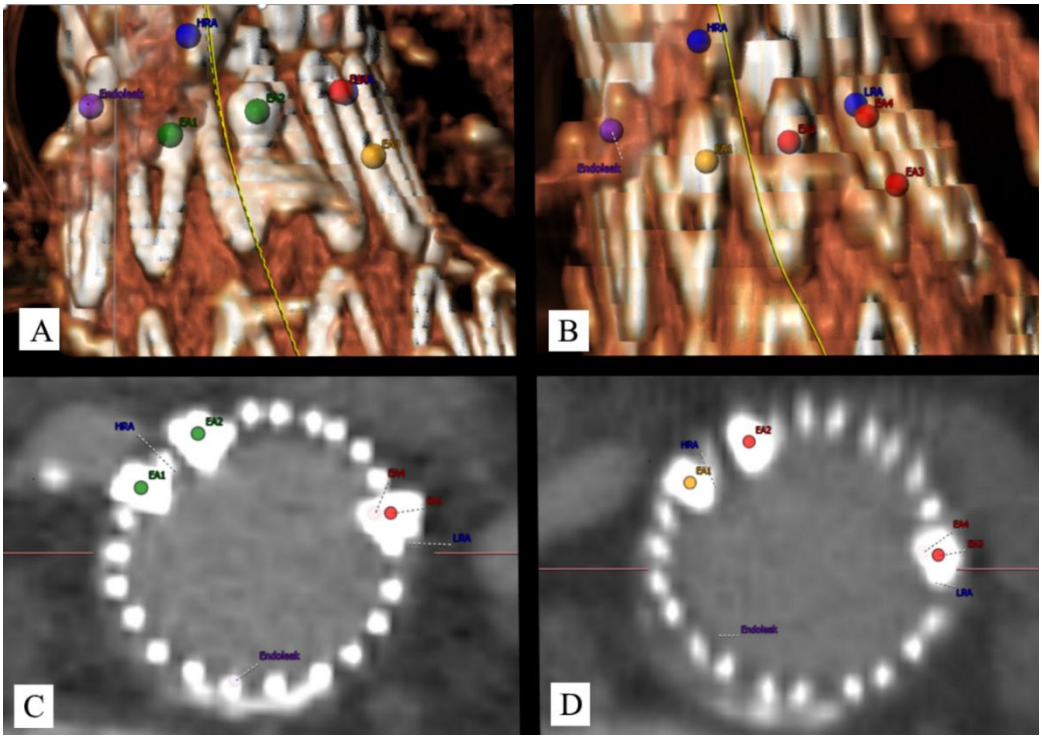

Figure 4. 3D (A, B) and axial (C, D) views of the distribution of EndoAnchor implants at the 30 days CTA scan (A, C) and the 11 months CTA scan (B, D). Good, borderline and non-penetrating EndoAnchor implants are visualized as respectively green, orange and red dots. EA1 and EA2 became respectively borderline and non- penetrating at the 11 months follow-up. Note that only 4 EndoAnchor implants had been implanted, unevenly divided around the aortic neck. The purple dot represents the location of the endoleak and the blue dots represent the locations of the highest and lowest renal arteries (respectively the HRA and LRA).

Table 3. Characteristics of the aorta, endograft and EndoAnchor implants where one EndoAnchor implant became borderline penetrating (Figure 5).

Characteristics		
Follow-up, months	34	
Endograft	Gore Excluder	
Size endograft, mm	28.5	
Oversizing, %	12.4%	
Number of EndoAnchor Implants	11	
	30 days CTA scan	*34 months CTA scan*
Good penetration, N	2	1
Borderline penetration, N	4	5
No penetration, N	5	5
Endoleak	Yes	Yes
Measurements		
Suprarenal aortic diameter, mm	27.1	26.0
Aortic diameter at lowest renal, mm	24.9	24.8
Aortic diameter 5-mm below lowest renal, mm	25.9	25.4
Aortic diameter 10-mm below lowest renal, mm	31.0	28.5
Proximal neck length, mm	6.5	8.0
Maximum sac diameter, mm	90.6	85.6
Suprarenal angulation, °	16	11
Infrarenal angulation, °	12	18
Infrarenal angulation to bifurcation, °	12	18
Neck thrombus average thickness, mm	0	0
Neck thrombus circumference, °	0	0
Neck calcium average thickness, mm	0	2
Neck calcium circumference, °	54	54

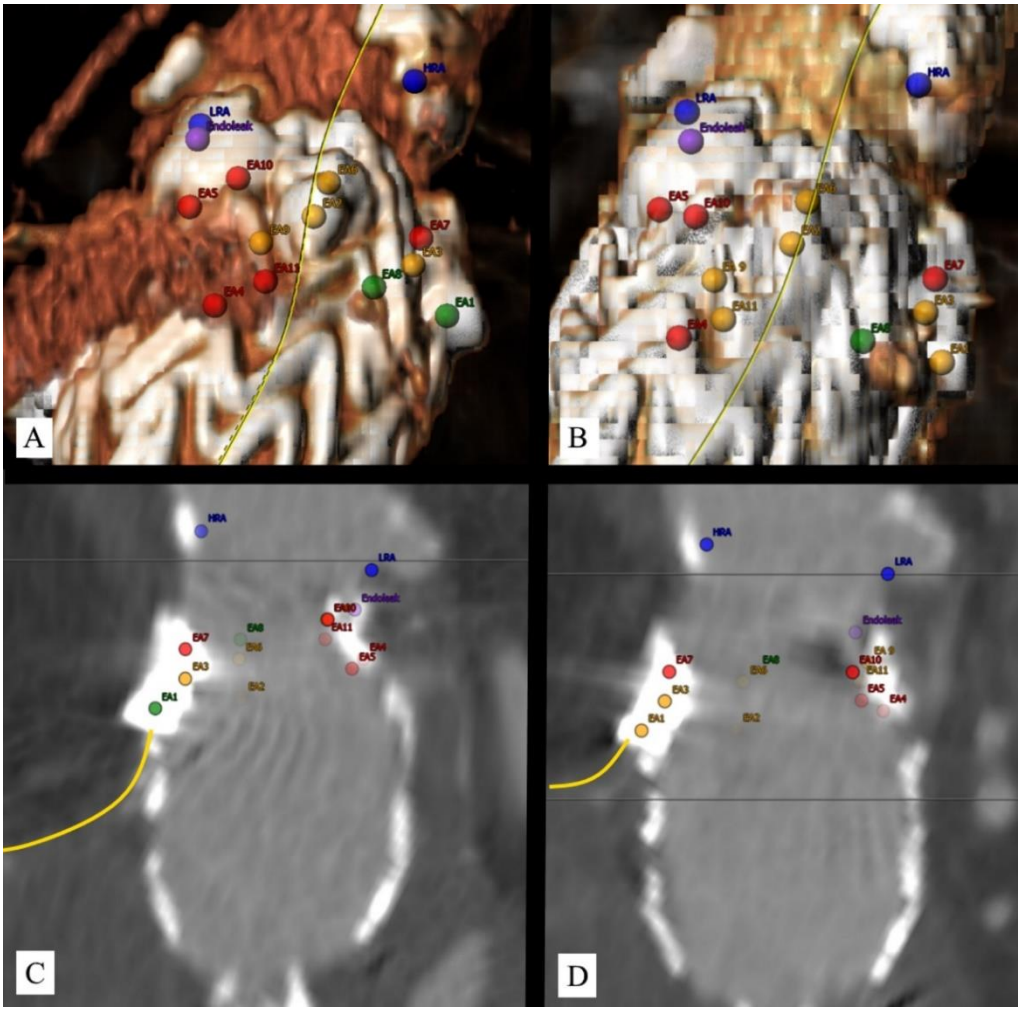

Figure 5. 3D (A, B) and longitudinal (C, D) views of the distribution of EndoAnchor implants on the 30 days CTA scan (A, C) and the 34 months CTA scan (B, D) (follow-up of 34 months). Good, borderline and non-penetrating EndoAnchor implants are visualized as respectively green, orange and red dots. The orange line accentuates the location of the aneurysm sac. The location of the endoleak is visualized with a purple dot. The blue dots represent the locations of the highest and lowest renal arteries (respectively the HRA and LRA). Note that only two EndoAnchor implants had a good penetration during initial implant. The majority of EndoAnchor implants were used beyond the recommended use.

Angle measurements

The median orthogonal angles of the good labelled EndoAnchor implants on the first postprocedural CTA scan and the last postprocedural CTA scan were 92 [IQR, 85-98] degrees and 90 [IQR, 84-97] degrees (P = 0.822), respectively. For the

longitudinal angles a median of 85 [IQR, 71-96] degrees and 84 [IQR, 70-96] degrees (first versus last postprocedural CTA scan) were found (P= 0.043). This resulted in a median difference of 1.0 [orthogonal angles; IQR, -7.0 - 7.0] and 2.0 [longitudinal angles; IQR, -6.0 - 9.0] between the first and last postprocedural CTA scan. Figure 6 and 7 show scatterplots of the differences between the angle measurements of respectively the orthogonal angles and the longitudinal angles.

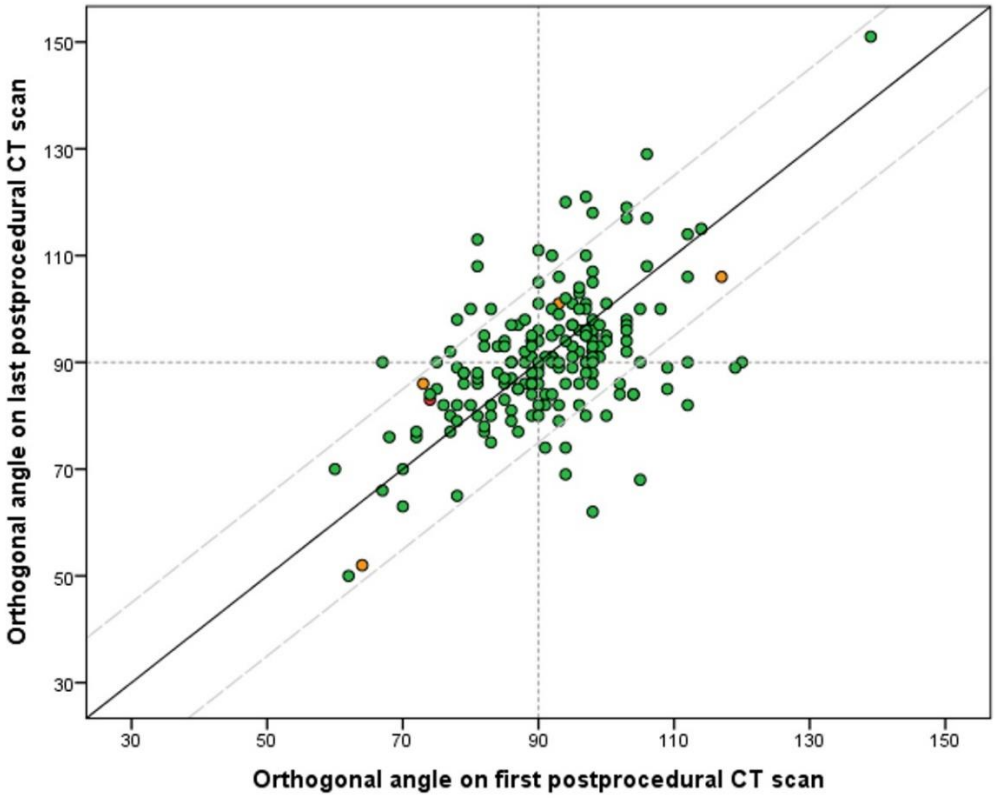

Figure 6. Scatterplot of the orthogonal angles at the first versus the last postprocedural CTA scan. The references line (bold black line) shows the EndoAnchor implants where the orthogonal angle remains the same on sequential CTA scans. The EndoAnchor implants between the two dashed grey lines represent the EndoAnchor implants where the difference between measured orthogonal angles is < 15 degrees. The 183 EndoAnchor implants which remain good penetrating are visualized in green. The four and one EndoAnchor implants which turn respectively borderline and non-penetrating are visualized in orange and red.

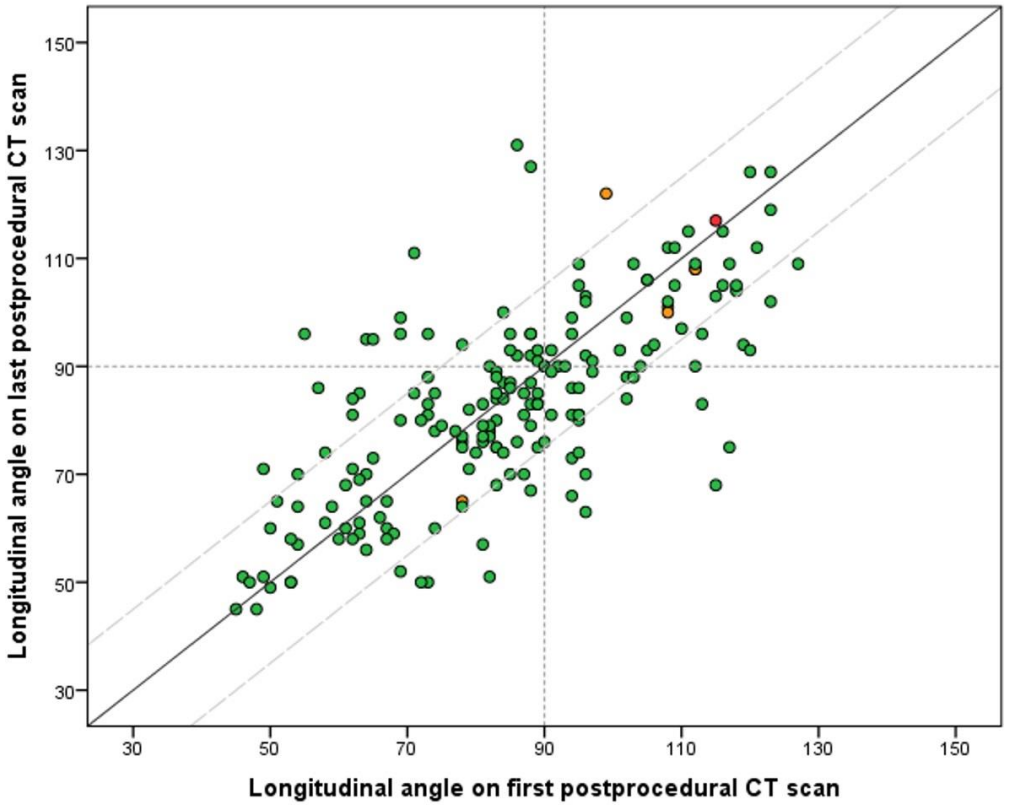

Figure 7. Scatterplot of the longitudinal angles on the first versus the last postprocedural CTA scan. The references line (bold black line) shows the EndoAnchor implants where the orthogonal angle remains the same. The EndoAnchor implants between the two dashed grey lines represent the EndoAnchor implants where the difference between measured orthogonal angles is < 15 degrees. The 183 EndoAnchor implants which remain good penetrating are visualized in green. The four and one EndoAnchor implants which turn respectively borderline and non-penetrating are visualized in orange and red.

2.5 Discussion

This is the first manuscript to analyse eventual changes in penetration depth and angles of EndoAnchor implants over time. At a median CTA scan follow-up of 13 months, no change in penetration depth was seen in 97.6% of 187 initially good penetrating EndoAnchor implants. Five of 187 EndoAnchor implants changed to borderline (n=4) or no (n=1) penetration, but without clinical sequelae.

The percentage of type IA endoleaks in this cohort is higher compared to previous one-year results from the ANCHOR registry[26] (respectively 35% vs 7%). Most

important reason is the fact that this cohort is a subcohort from the ANCHOR registry. In this cohort, only patients treated therapeutically for a type IA endoleak without any other adjunct other than EndoAnchor implants (i.e. cuffs or chimney extensions) are included.

Despite the persistence of a type IA endoleak in eighteen patients, the mean aneurysm diameter decreased significantly. This is in line with previous findings of a matched cohort comparison in patients with and without EndoAnchor implants.[29] Persistent type IA endoleaks seem to be mild, without high-flow. This might be due to the resistance of the good positioned EndoAnchor implants against the pressure of the endoleak between the aortic wall and endograft. Moreover, in six patients the type IA endoleak resolved spontaneously on follow-up, probably due to the low flow endoleak and thrombus formation in the small gutters.

This subcohort showed a maldeployment in 48% of all the initial deployed EndoAnchor implants compared to 29% in a previous study limited to the one-month CTA scans.[28] In this analysis, relatively more EndoAnchor implants were deployed beyond the recommended use. They were positioned in the aneurysm sac or at a location where there is a gap between the aortic wall and endograft.

One should keep in mind that an EndoAnchor implant cannot unscrew itself off the aortic wall. If an EndoAnchor implant is positioned according to the recommended use and no forces are applied on the EndoAnchor implant between the aortic wall and endograft, the implant will be unlikely to change position over time. When a gap occurs between the fabric and the aortic wall above the location of the EndoAnchor implants, only then might this implant be at risk to change position, as illustrated in Figure 8. Therefore, it is important to position the EndoAnchor implant as proximal as possible to the endograft fabric edge. If a gap does occur, one might need to position a cuff to resolve the gap between the endograft and aortic wall.

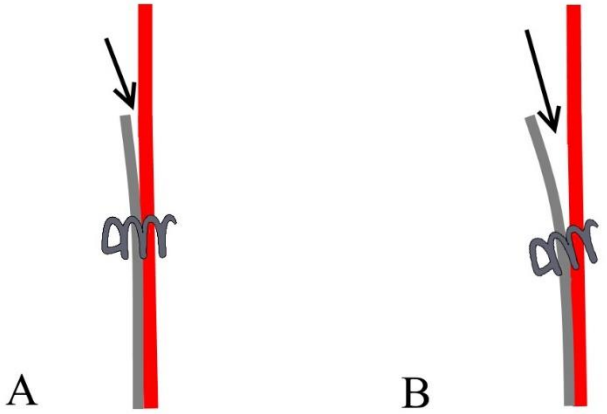

Figure 8. Longitudinal schematic representation of the increase of a gap between the aortic wall (red line) and the endograft (grey line). A) The EndoAnchor implant is penetrating the aortic wall, however, there is a space between the aortic wall and the endograft proximal of the EndoAnchor implant. B) Over time, the gap at the proximal edge of the endograft increases due to the pressurization of the gap. This may cause the EndoAnchor implant to become borderline or even non-penetrating.

There is a significant difference between the longitudinal angles on the first and last postprocedural scans. An explanation can be found in the large deviation between all measured EndoAnchor implants. Moreover, the aorta is a dynamic environment and the orientation of the EndoAnchor implants might change during the cardiac cycle. The CT scans were static images, and no dynamic imaging was performed to assess the differences in penetration angles. Due to this uncertainty in measurements, a small change in EndoAnchor implant penetration angle does not result in any clinical impact. This is in line with our previous study on EndoAnchor implant penetration angles.[28] Most of the EndoAnchor implant penetration angles were within ±15 degrees change, which has no impact on outcome.

These results show that when EndoAnchor implants are successfully positioned they will most likely remain successful over time. It is therefore important to have a good initial positioning of the EndoAnchor implant. To do so, pre- and peri-procedural planning and techniques need to be carefully executed.[27] First, preplanning of the procedure is important. The aortic neck needs to be inside the recommended instructions for use for optimal positioning. Moreover, oversizing of

the endograft needs to be between the 15-25% in order to have good apposition of the endograft, without the risk of infolding. Infolding increases the risk of gaps between the aortic wall and endograft, which cannot be solved with EndoAnchor implants.

Second, the radius of the endoguide needs to match the diameter of the aortic neck to ensure technical success in positioning of the implants. Furthermore, the position of the C-arm relative to the endoguide and EndoAnchor implants needs to be perfectly perpendicular to visualize the proper penetration angles. Moreover, all this requires practice. So, the learning curve of the physician needs to be considered.

2.5.1 Limitation

This study included a small cohort of patients with only 13 months follow up. No dynamic CTA scans were available, only static CTA scans were used. Therefore, changes in EndoAnchor implant penetration and angles during the cardiac cycle were not measured. It might be interesting to investigate the imaging of EndoAnchor implants during the cardiac cycle.

2.6 Conclusion

Sustainability of individual EndoAnchor implants is excellent. A total of 97.4% of the good penetrating EndoAnchor implants remained good at a median follow-up of 13 months in patients with a substantial amount of hostile infrarenal necks. Only five EndoAnchor implants became borderline or non-penetrating without any clinical consequence. This analysis emphasizes the utmost importance of delivering EndoAnchor implants accurately and effectively through the aortic wall.

3. Validation of an *in-vitro* setup to investigate the effect of EndoAnchor positioning on migration resistance of an endograft

3.1 Introduction

According to the Instructions For Use (IFU) of the EndoAnchors, it is recommended to distribute them evenly around the circumference of the sealing endograft. The minimum number of EndoAnchors to be deployed depends on the native vessel diameter, vessel angulation and endograft type (bifurcated or tube) and is independent of the amount of endograft oversizing.[30] However, clinical experience also reveals EndoAnchor usage beyond the recommended use. For example, EndoAnchors are sometimes deployed only at the location of the endoleak, opposite to each other in the vessel wall, or to attach two endografts to each other. To investigate the effect of this EndoAnchor positioning, an *in-vitro* model will be developed and validated.

Recent studies indicate that penetration and configuration of EndoAnchors can influence the clinical outcome.[22,28,31] A follow-up study showed that the position and penetration in 97.4% of the EndoAnchors did not change over time. Thorough analysis of the follow-up data identified differences in distribution patterns besides the recommended use. The consequences of these distribution patterns are still unknown.[31] It is plausible that there is a correlation between the distribution and penetration of EndoAnchors and migration of the endograft (i.e. the areas where there are no EndoAnchors). This may affect the clinical outcome of these patients, by for example the increased risk of type IA endoleaks. However, this is difficult to determine in a clinical setting because multiple variables can influence the outcome. Therefore, it is necessary to examine the effects of different EndoAnchor configurations on migration resistance of an endograft in a controlled environment.

The aim of this chapter is to investigate what kind of measurement setup can provide a validated environment where the effect of the positioning of EndoAnchors on endograft migration can be tested with pulling force in silicon models. The requirements for such a measurement setup will be described and tested for validation.

3.2 Method

3.2.1 Materials and requirements

There are several requirements that a setup must meet to investigate the effect of EndoAnchors positioning on endograft migration with tensile force in silicon models. First, a model that mimics the situation of the endograft within the aortic

vessel must be created; this will be done with an endograft and a silicone tube. Second, forces need to be applied on the endograft to mimic the forces in the human body. This can be done with a pulling mechanism that is attached to the endograft and is displaced by a motor. The applied forces will be measured with a force sensor. An Arduino Mega 2560 board will interface all these components and a computer will control the Arduino.

An important aspect of the measurement setup is to visualize what happens with the endograft, EndoAnchors and silicon tube when experiencing pulling forces. When these forces are induced, it is essential to view the entire proximal zone of the endograft to visualize migration of the endograft and EndoAnchors. Therefore, a 360-degree view will be created within the endograft with a camera and a mirror cone. For additional information, a second camera will be positioned next to the model to record the changes visible from the outside of the setup.

In the end, the following requirements should be met for the measurement setup; control the entire measurement with software (developed in MATLAB 2015b), film the measurement setup with two cameras, read the force sensor and actuate the motor to induce forces on the endograft. The complete list with materials and requirements are listed in appendix B.

3.2.2 Test protocol

Every component of the setup was tested to determine whether they met the requirements necessary to gather all the information during the entire measurement and if the measurements could be performed in a controlled manner. Five tests were performed to calibrate and validate the entire setup. The description, requirements and performance of these tests can be found in appendix C.

Test 1: Calibration of the force sensor

The force sensor required calibration to determine the agreement between the force displayed by the sensor and the actual force that was applied. In order to validate this, several weights were measured to verify their actual mass, and were subsequently attached to the force sensor for calibration. This calibration also allowed us to determine the performance of the Arduino and MATLAB regarding the force sensor.

Test 2: Calibration of the camera view of the cone
The 360-degree view was constructed by filming a mirror cone with a camera. This view was slightly distorted by the cone shape and thus it is paramount that the amount of elongation was determined to relate the acquired images to reality. Therefore, a calibration pattern on squared paper was placed in the area viewed with the mirror cone. In this way, the amount of endograft migration can also be determined with the inner camera. However, the outside camera is the principle method to determine the amount of migration.

Test 3: Testing the functionalities of the silicon tube
During the measurements, the endograft, EndoAnchors and silicon tube will experience forces that can result in changes to one or multiple components. Therefore, it is necessary to know the individual characteristics of the silicon tube when it experiences the force. To analyse this, the pulling mechanism was attached to the tube. Thereafter, force was induced and increased to 100 N. This was done for three different settings: the tube marked with a dot and a 5 mm incision made in longitudinal and orthogonal direction in the silicon tube. This allowed us to investigate the characteristics of the silicon tube under several conditions.

Test 4: Testing the functionalities of the measurement setup
All components and requirements were tested by inserting a dummy endograft in the setup and carrying out the measurement. A needle was inserted transversal through the silicon tube and endograft to simulate the anchoring of an EndoAnchor. These measurements were repeated until all the functionalities and boundary conditions were determined and finalized.

Test 5: Determine if the EndoAnchors are reusable
Durability test of the EndoAnchors were previously performed and showed minor hole elongation at the location of the EndoAnchor. This occurred between the 300 and 400 million heart cycles. For these tests, endografts comparable to the Valiant thoracic stent graft (i.e. same graft material and construction) were used. These measurements were performed under severe test conditions (worst-case axial loading), but still no tearing of the fabric or pulling out of the EndoAnchor was observed. Therefore, it can be assumed that the endograft with the same deployed EndoAnchor(s) can experience force multiple times.[30]

Nevertheless, durability tests for EndoAnchors within this setup were performed to determine whether exposing the EndoAnchor to the same force several times alters the EndoAnchor's functioning. In this way, the efficiency of the measurements will be increased. An Endurant endograft (25 mm diameter, thus no oversizing) was deployed with one EndoAnchor during the durability tests. To assure the durability of EndoAnchors during the measurements in this *in-vitro* setup, the EndoAnchor endured the same measurement 50 times. If these measurements showed no sustainable difference in the endograft migration force, the EndoAnchors were considered to be reusable for the actual measurements. Otherwise, new EndoAnchors had to be deployed every time we performed another step in the measurement protocol. Thus, these measurements were not representative for the actual EMF values, because there was no oversizing of the endograft.

Final validation

The setup was initially calibrated and validated with an Endurant endograft, as explained in the previous paragraphs. In the final part of the validation, the setup was once more tested with the Valiant endograft. This final test will make sure that the calibration and validation were still accurate with a different endograft. Thereafter, baseline measurements were performed with the Valiant endograft, which will be used for all following measurements.

The baseline measurement involves generating forces on the endograft until changes occur to the endograft, EndoAnchors or silicon tube. The force necessary to migrate the endograft 3 mm was defined as endograft migration force (EMF). The measurement will be terminated by visual examination after achieving the 3 mm migration or by the built-in safety in the software (that will automatically stop when a force decay of 2 N is observed). The baseline measurements will be performed five times with the Valiant endograft without EndoAnchors to determine the baseline EMF. The median of the baseline EMF can be used to determine the relative effect of deploying several EndoAnchors in several configurations on endograft migration.

3.2.3 Statistical analysis

All measurements are performed five times, because early tests show consistent results during the same conditions. The data is assumed to be non-normally distributed, and hence data will be expressed as median [IQR].

3.3 Results

The final measurement setup including all components that meets all the requirements is displayed in Figure 9.

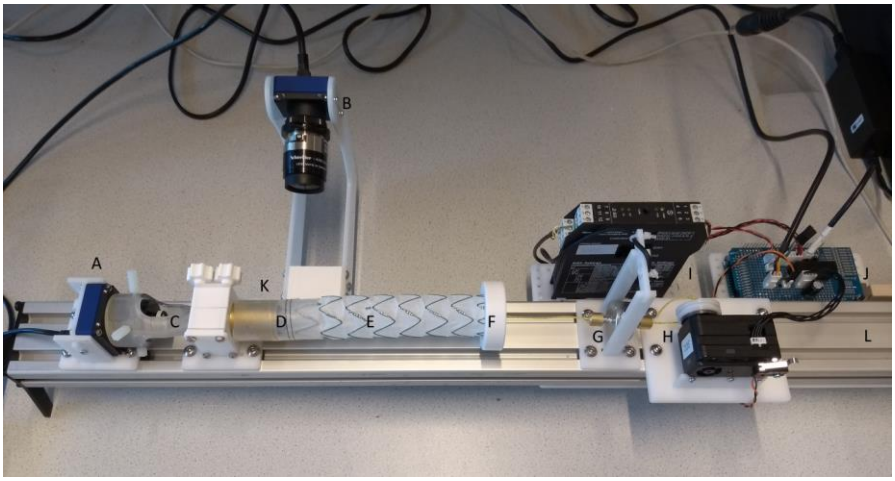

Figure 9. An overview of the measurement setup; the measurement setup contains camera 1 (A), camera 2 (B), lens holder (C), mirror cone (D), endograft (E), pulling plug (F), force sensor (G), motor (H), force sensor converter (I), Arduino Mega 2560 (J), the silicon tube (K) and a rails (L) to mount all the components

3.3.1 Test 1: Calibration of the force sensor

Figure 10 shows the results of the calibration of the force sensor. Several weights were measured twice with the force sensor, which is illustrated with the orange and blue line. Overall, the correlation between the force sensor value and the measured weight is linear, resulting in a successful calibration.

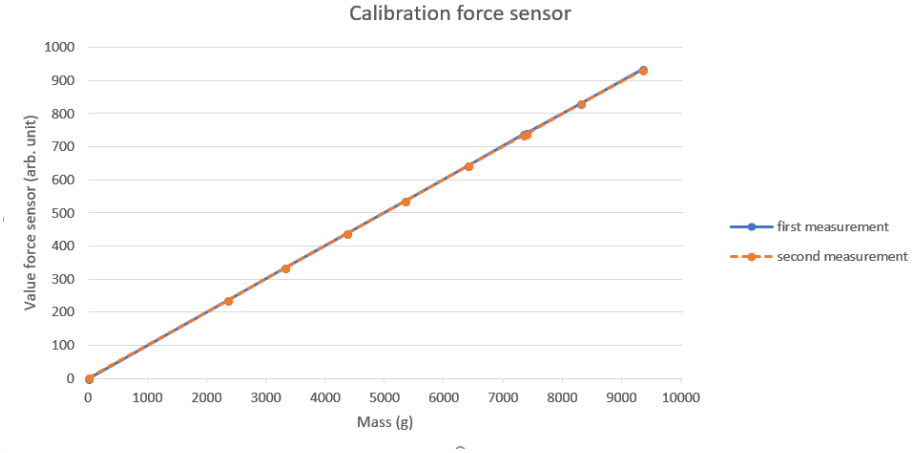

Figure 10. The trendline of the force sensor calibration

3.3.2 Test 2: Calibration of the camera view of the cone

Figure 11 explains the camera view of the mirror cone. Here, Figure 11a is a schematic view of the setup around the mirror cone and Figure 11b is the camera view of the mirror cone. The orange and purple dots correspond to the locations of the mirror cone and the location within the camera image. The middle part of the camera image (*orange dot*) corresponds to the most proximal part of the mirror cone and thereby the endograft. The outer part of the camera image (*purple dots*) can be related to the most distal part of the mirror cone and thereby the endograft. Thus, the camera view ranges between the top and distal parts of the mirror cone (5 mm length). The orientation of the camera corresponds to the orientation of the cone, e.g. where the upper part of the image matches with the upper part of the cone. If the endograft is migrating, this will start from the middle to the outer part in the camera image.

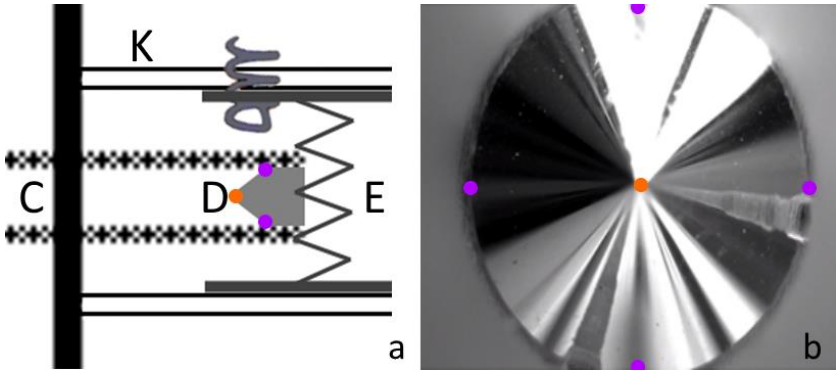

Figure 11. Representation of the mirror cone and camera view. a) A schematic depiction of camera 1 within the silicon tube (K) and endograft (E). The mirror cone (D) is fixed by the lens holder (C). The top of the mirror cone is represented by the orange dot, and the outer part (furthest point) with purple dots. b) View of the camera onto the mirror cone with the corresponding points (orange and purple dots)

The elongation of the mirror cone is determined by placing a calibration pattern created with a black (Figure 12a) and blue pencil (Figure 12c) within the silicon tube around the cone within view of the camera (between orange and purple dots, Figure 11a). The resulting camera images show no noticeable differences (Figures 12b and 12d). However, the circles are visualized as ellipses on the camera images. Furthermore, Figures 12b and 12d show that mirror cone illustrates a distorted image, where 1 mm covers a larger area of the image at the outer parts (*orange*

lines) than at the inner part (*blue lines*) of the cone. This results in a bigger angulation of the line in the middle than at the outer part.

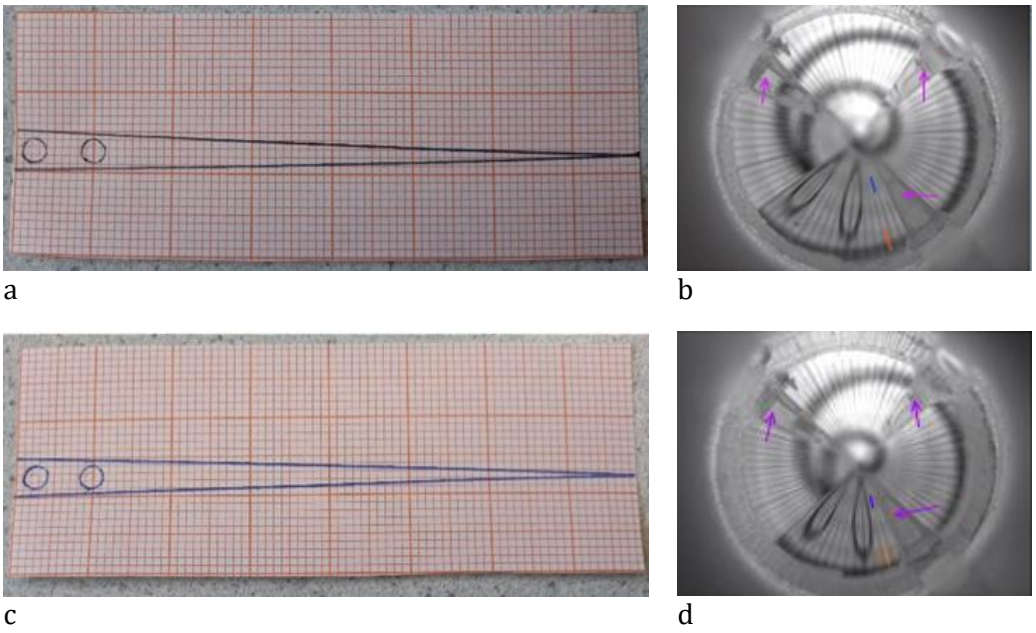

Figure 12. The resulting images of the calibration of the cone elongation with both calibration patterns (a, c) and the corresponding images with the camera (b, d). Note the three lines (purple arrows), which are fixation mechanism of the mirror cone with the lens holder.

3.3.3 Test 3: Testing the functionalities of the silicon tube

Three conditions were created; a black dot on the silicon tube (Figure 13.1), a longitudinal incision in the silicon tube (Figure 13.2) and an orthogonal incision in the silicon tube (Figure 13.3). Both incisions were 5 mm of length. Every condition was divided into three phases; the silicon in rest with no applied force (Figure 13.a), the silicon tube experiencing 100 N force (Figure 13.b) and the silicon tube after force had been applied (Figure 13.c). The red arrow shows the direction of the applied force in Figure 13.b. A few observations can be made when evaluating these images. First, it is interesting to observe the elasticity of the silicon when experiencing force, which results in displacement of the dot or incision to the right towards the direction of the force (Figure 13.b). This also results in a minor stretching (approximately 2 mm) of the dot and longitudinal incision and in a gap in the orthogonal incision. However, Figure 13.3b shows that the orthogonal incision teared due to the applied pulling force. This happened at approximately 90

N. Figure 13.c show that the other conditions revert to the rest state when the force was released, where the longitudinal incision did not expand.

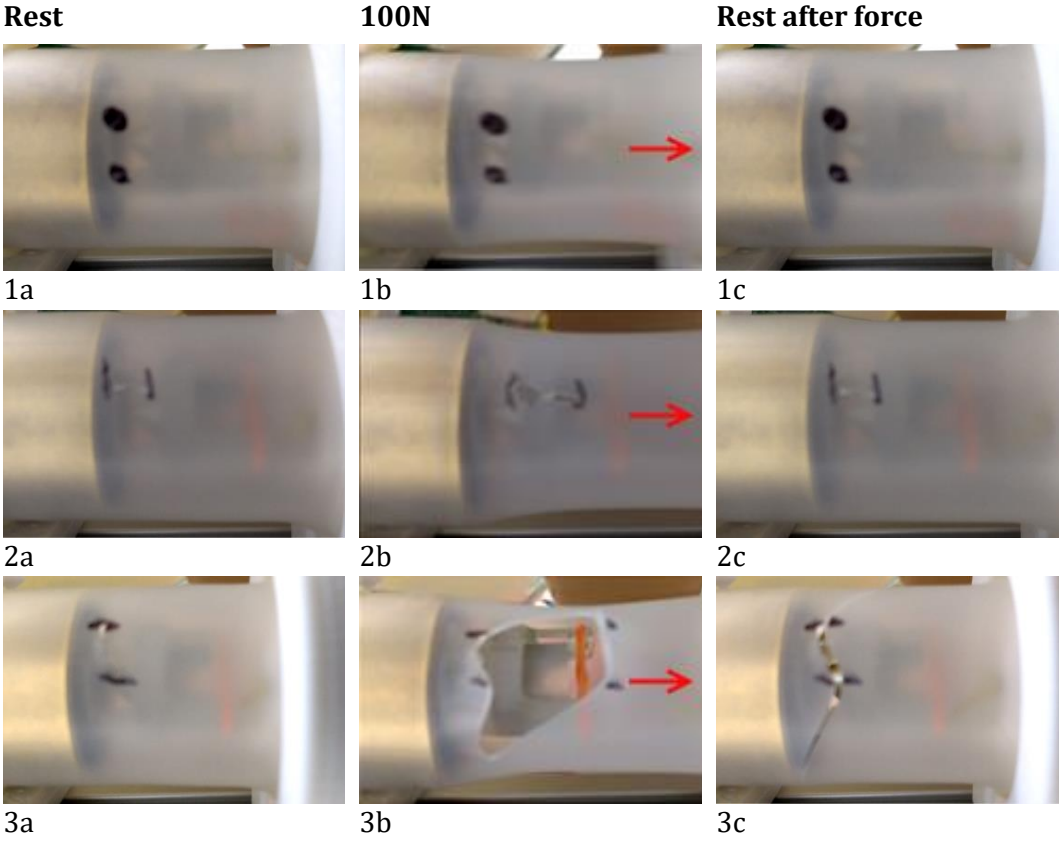

Figure 13. Results of different test conditions with the silicon tube; (1) a dot drawn on the silicon tube, (2) longitudinal incision, and (3) orthogonal incision. (1-3a) silicon in rest state, (1-3b) a maximum force of 100 N is applied (red arrow), and (1-3c) the applied force is released, and silicon returns to a state of rest.

3.3.4 Test 4: Testing the functionalities of the measurement setup

The measurement setup is tested by placing a needle (Figure 14a and 14b, *red arrow*) through the endograft and silicon tube to create two anchoring locations. Figure 14 shows the results of these measurements, where the boundaries of the endograft are visualized with the red circle or line. The inner camera (Figure 14a and 14b) illustrates the asymmetric movement of the endograft after applying force. The part of the endograft opposite to the needle placement has moved. This is also observed with the second camera (Figure 14c and 14d).

Endograft at 0 mm migration **Endograft at 3 mm migration**

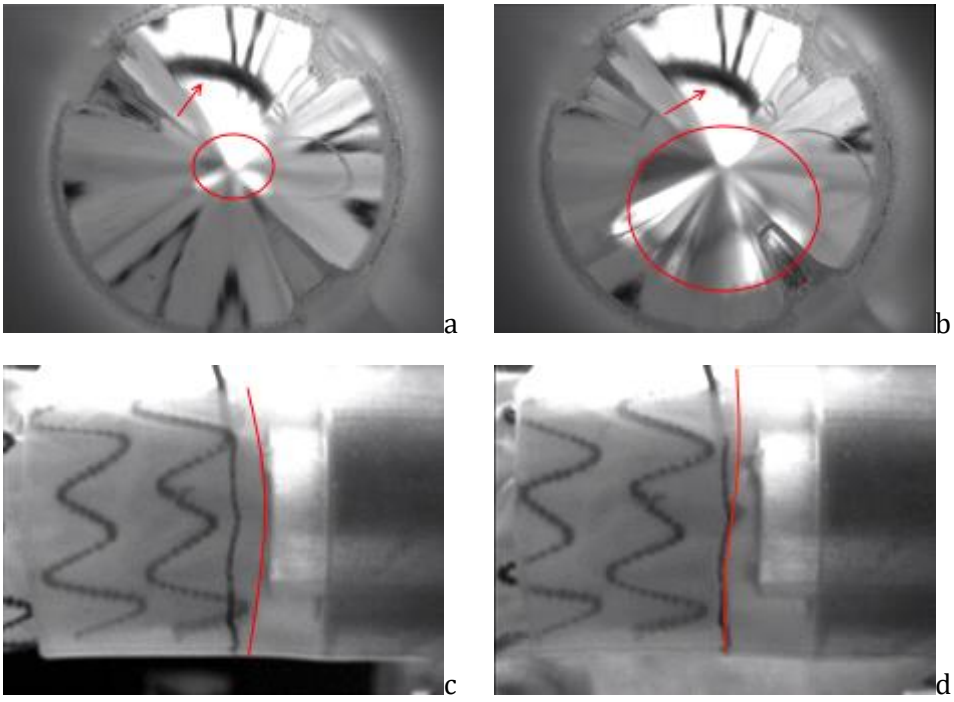

Figure 14. Visualization of the test with the 360-degree camera view (a, b) and the outside camera (c, d) with the starting point (a, c) and the end point (b, d) of the measurement, where the needle is highlighted with the red arrow and the proximal zone of the endograft is highlighted with the red line.

These measurements have shown and tested the functionalities of the setup. When the requirements of the setup are evaluated, the following checks can be made:

- ✓ Camera is functioning
- ✓ Force sensor needs to show reliable results
- ✓ The Herkulex servo module is functioning, thus the motor can apply force on the endograft and is controlled with the Arduino and MATLAB software
- ✓ Arduino is functioning, thus the computer can communicate with the Arduino to control and read all the components of the measurement setup
- ✓ Silicon tube needs to simulate the aortic wall and needs to resist forces which are applied on the tube
- ✓ The fixation of the endograft must be comparable to the conditions of the endograft in the body
- ✓ MATLAB should be functioning to control the measurement setup

3.3.5 Test 5: Determine if the EndoAnchors are reusable

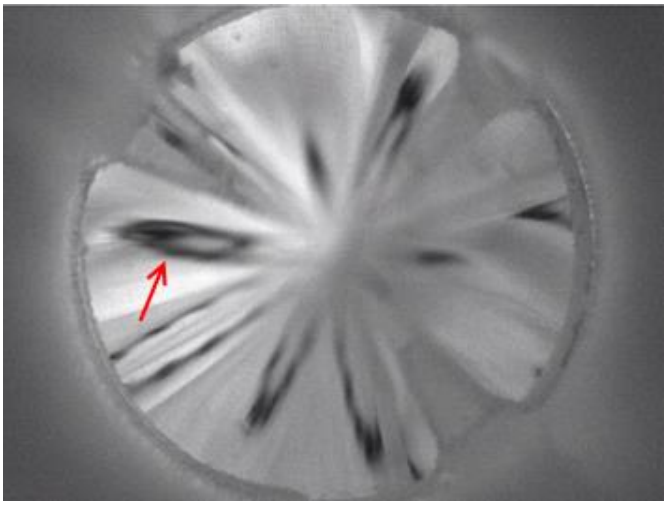

Figure 15. Illustration of EndoAnchor placement in the endograft during the durability tests for this setup

Figure 15 shows the position of an EndoAnchor in the endograft during the durability tests for an EndoAnchor in this setup. These tests were performed 50 times and resulted in a median EMF of 4.20 N [4.11-4.30 N] with an Endurant endograft with no oversizing.

3.3.6 Baseline measurement

The baseline measurement resulted in a median EMF of 4.99 N [4.69-4.99 N]. Figure 16 presents a visualization of the endograft during the measurement. Figure 16a and 16c show the position of the endograft at the starting point and Figure 16b and 16d show the position of the endograft after movement. The outside camera (Figure 16c and 16d) depicts the migration of the endograft (Figure 16.a and 16c, *red arrows*) and the stretching of the silicon tube, especially at the lower part of the tube. The inside camera (Figure 16a and 16b) presents a circumferential movement of the endograft during the measurement, where the mirror becomes more circumferential visible at the end point of the measurement. The final position of the endograft is visualized by the red lines in Figure 16b and 16d.

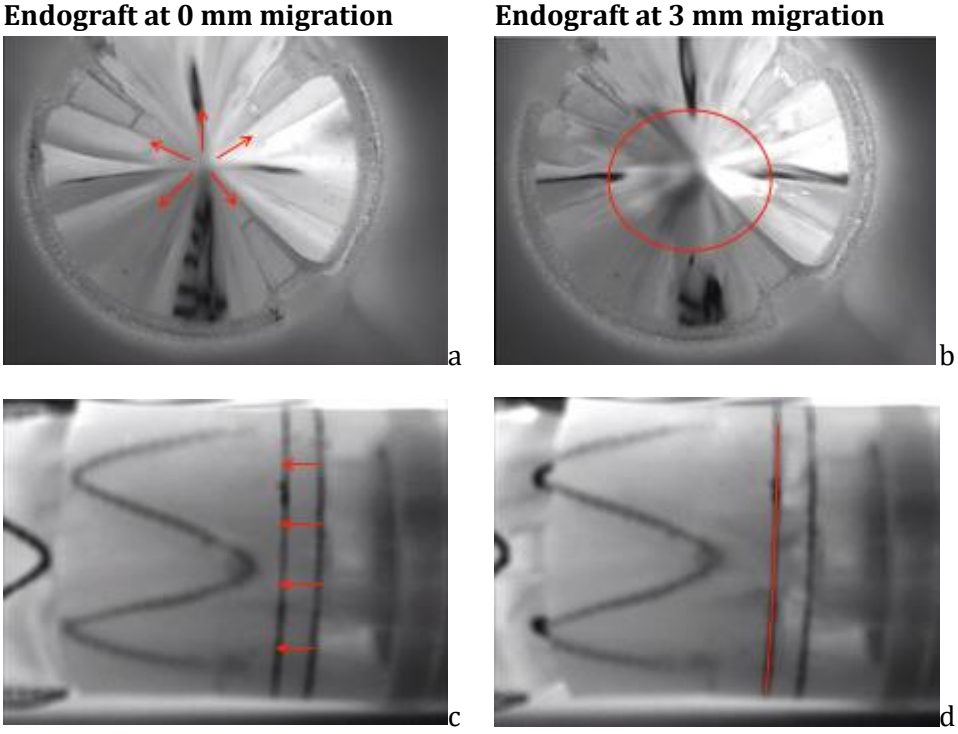

Figure 16. Visualization of the baseline measurement with the 360-degree camera view (a, b) and the outside camera (c, d) with the starting point (a, c) and the end point (b, d) of the measurement

3.4 Discussion

This chapter aimed to investigate which measurement setup can provide a validated environment where the effect of the EndoAnchor positioning on endograft migration can be tested. After evaluating the requirements, a setup was created and validated.

The calibration of the force sensor demonstrated a linear correlation, resulting in a simple conversion of the force sensor value to an actual force. Furthermore, the cameras were tested to determine whether they would meet the predefined requirements and the inner camera was calibrated to determine its elongation. One camera was placed on the outside of the setup to determine if changes to the EndoAnchor, endograft and/or silicon tube occurred. This camera was facing the location, where some of these changes were likely to occur. Since the other parts of the setup were not recorded from the outside, an improvement would be to implement a second camera there. Nonetheless, the inner camera already records

the 360-degree view of a part of the setup, which should be sufficient to obtain all the necessary information during the measurements.

Subsequently, the silicon material was calibrated. The calibration of the silicon has proven to be reliable for the measurements. At first, we intended to use another silicon sample with a 2 mm wall thickness. However, this sample appeared to have a high resistance during the tests, resulting in a failed EndoAnchor deployment (e.g. breaking or distortion). Thus, a silicon sample with a 1 mm wall thickness was tested further with the intention to use for the measurements. This silicon sample teared, when experiencing a force of 90 N. However, this is far beyond the force necessary to tear the aorta. Thus, this silicon is sufficient to use. More effort could have been given to finding a better reflection of the reality, resulting in a more reliable type of silicon. Subsequently, animal material could be considered as an alternative material. However, the defined migration cannot be determined then because the material is not transparent. Furthermore, this is also beyond the scope of the forthcoming study, where the relative effect of EndoAnchor placement will be investigated and not the absolute effect. Therefore, the material choice for this purpose is considered to be sufficient when the following requirements are met; easily obtainable, flexible enough to provide EndoAnchor deployment and sufficiently strong to experience forces without tearing. All these three requirements were met by the final sample of silicon.

Furthermore, the EndoAnchor reusability within this setup was investigated. It should be noted that the resulting EMF of these tests are not comparable to the performed baseline measurement. During these test, an endograft is used creating no oversizing and thereby a different setup than within the baseline measurements. The reusability tests demonstrated consistent results, not indicating changes within the EndoAnchor material. This corresponds to the results demonstrated by Han et al. (2002)[32], describing the properties of the EndoAnchor material. The authors determined a minimal yield strength of 2000 MPa at room temperature, being equivalent to 2000 N/mm^2. An EndoAnchor has a diameter of approximately 0.5 mm, which results in a surface of 0.19 mm^2. Thus, the maximum load of an EndoAnchor is 393 N, prior to the occurrence of plastic deformation of the material. This amount of force is six times larger than the maximum force intended to be applied during the measurements, since the aortic material tears at a force of 56 N.[20] Previously performed durability tests also

confirmed the strength of an EndoAnchor.[30] In conclusion, EndoAnchors are reusable for multiple measurements.

Another part of the setup was the software, which consisted of two parts; first, the software on the Arduino to interface and control the different parts of the setup and second, the MATLAB software to control the Arduino with the computer. The software was tested extensively to determine whether the basic performances of the measurements were achieved. However, a fully automatic performance of the software would be desirable. In that case, more in-depth analyses of force decay could have been performed to implement a more sophisticated automatic stop, in case of endograft migration. Furthermore, only one software program controlling the measurements is desired. This could be achieved by implementing the full initialization of the Arduino in MATLAB. Nonetheless, these optimisations are small improvements to create a better software connection and thereby increasing the user-friendliness of the software. In the current situation, the software provided accurate information to perform and analyse the measurements.

Finally, an improvement to the setup could be to integrate a display within the camera view to show the applied force during the measurement. In the current setup, the videos cannot be directly related to the force at that point in time. Analysing the videos, it is desirable to see also the amount of applied force. However, the focus will be on the force applied at 3 mm migration in the forthcoming study, which is known when the measurement is terminated.

3.5 Conclusion

In conclusion, a setup was created which met the predefined requirements. It can be used to investigate the effect of EndoAnchor positioning on endograft migration. The different parts of the setup were tested and demonstrated to function within the required ranges.

4. The effect of different EndoAnchor configurations on proximal endograft migration resistance: an *in-vitro* study

4.1 Abstract

Objective: The aim of this study was to investigate the effect of different EndoAnchor configurations on proximal endograft migration resistance when a constantly increasing force is applied within an *in-vitro* measurement setup.

Methods: A setup was developed and validated to perform force measurements on different EndoAnchor configurations within an endograft and silicon tube. Four different configurations (i.e. circumferential with six EndoAnchors, five EndoAnchors within 120 degrees with one EndoAnchor at the opposite part, four EndoAnchors opposite to each other, and two lines of three EndoAnchors) were deployed on the proximal sealing zone of the endograft with the silicon tube. These configurations were investigated by applying a constant pulling force at the distal end of the endograft. The force, necessary to displace the endograft 3 mm, was defined as the endograft migration force (EMF). The measurements were terminated when damage or 3 mm endograft migration was observed or 60 N was reached. The measurements were recorded by two cameras and later analysed to determine whether changes or damage to the EndoAnchors, endograft or silicon tube had occurred.

Results: The main result was the influence of distance between EndoAnchors on the migration resistance of the endograft. Median EMF was 42.4 N [41.4 – 46.8 N], 29.0 N [28.9 – 29.7 N], 24.6 N [24.1 – 27.1 N], and 9.6 N [9.5 – 9.8 N] for respectively the circumferential, EndoAnchors within 120 degrees, EndoAnchors opposite to each other, and two lines of each three EndoAnchors configuration. The influence of six EndoAnchors in comparison to five EndoAnchors in a circumferential configuration showed a difference of almost 35 N in EMF.

Conclusion: This study demonstrates the migration behaviour of the endograft within different EndoAnchor configurations, where distance between EndoAnchors and circumferential deployment have shown to be important factors in creating a large migration resistance. The endograft remains relatively sensitive to migration if there is no circumferential deployment. Furthermore, deployment of a second row of EndoAnchors could also contribute to an increased migration resistance of the endograft.

4.2 Introduction

The Helix-FX EndoAnchor System (Medtronic Vascular, Santa Rosa, CA, USA) was developed to improve the sealing and fixation of an endograft after an endovascular aneurysm repair (EVAR) procedure.[14,20,27] EndoAnchors are designed to be deployed atraumatically through the endograft and vessel wall.[30] Additionally, the helical design allows for a safe fixation of the endograft to the aortic wall and minimizes the risk of perforation of adjacent structures. When EndoAnchors are deployed successfully and circumferentially in the aortic neck, the fixation strength can approximate the strength of a surgical hand-sewn anastomosis.[20,22,27,28] EndoAnchors can be used prophylactic to prevent migration and type IA endoleaks, while therapeutic use can treat acute and late type IA endoleaks. However, complications like migration can infrequently occur after EndoAnchor deployment.[25,26]

Goudeketting et al.[22] observed a correlation between successful EndoAnchor penetration and aortic neck characteristics in patients with type IA endoleaks. They demonstrated that the diameter and the amount of calcium in the aortic neck were independent predictors for EndoAnchor failure. Van Noort et al.[31] demonstrated that the durability of the individual EndoAnchor during follow-up was excellent. EndoAnchor penetration and deployment angles remained the same for 97.4% of all EndoAnchors during a median follow-up time of 13 months. Although not significant, the other 2.6% of the EndoAnchors showed a difference in angles and penetration, thus resulting in a larger number of borderline or non-penetrating EndoAnchors. A recent study of a selected cohort of the ANCHOR database showed that almost 30% of the EndoAnchors were maldeployed (i.e. EndoAnchor deployment above the fabric or at a location where the endograft lost apposition with the aortic wall).[28] Additionally, technical errors during deployment can result in larger angles between the EndoAnchor and the aortic wall, thereby increasing the risk of non-penetration of the EndoAnchors. Earlier studies highlight the importance of circumferential distribution of the EndoAnchors to achieve the intended migration resistance.[18,20,22,28,31,33] Various combinations of EndoAnchor penetration and distribution can influence the combined EndoAnchor functionality and endograft fixation strength. For example, it is plausible that one-sided EndoAnchor fixation may result in shifting of the endograft on the contralateral side. *In-vitro* studies with silicon models have proven to be effective in assessing knowledge about endograft fixation and displacement.[34,35] Furthermore, other studies investigated fixation and displacement of endograft

with EndoAnchors in experimental models.[20,36] Melas et al.[20] analysed the displacement force necessary to dislocate the endograft 20 mm when either 4 or 6 EndoAnchors were deployed circumferentially. In practice, circumferential distribution of EndoAnchors is not always achieved or intended[24,37,38]. However, the migration behaviour of endografts remains unclear when EndoAnchor distribution is other than circumferential. It is important to know the consequence of non-circumferential EndoAnchor deployment, as it can result in complications such as type IA endoleaks or endograft migration.[23,26] Therefore, the aim of this study is to investigate the effect of different EndoAnchor configurations on proximal endograft migration resistance when a constantly increasing force is applied.

4.3 Method

4.3.1 Model

A silicon tube (Peter van den Berg Afdichtingstechnieken B.V., VMQ 60˚ Shore A) with a wall thickness of 1 mm and a diameter of 24 mm was used to mimic the aortic wall in this *in-vitro* setup. Herein, a Valiant Thoracic Stent Graft (Medtronic) with a diameter of 30 mm was placed to create a 25% oversizing of the endograft. The endograft was deployed to generate a 20 mm sealing zone.

4.3.2 In-vitro setup

An in-house built *in-vitro* setup (Figure 17) was used to perform the pulling force measurements on the model. A computer controlled the measurement setup using dedicated software developed in MATLAB 2015b. Inside the tube, a camera (Matrix Vision, mvBlueFox-IGC2bG; FOV, 10×10 mm; FPS=12.3) filmed a mirror cone, which created a 360-degree view of its surrounding structures, e.g. silicon tube with endograft (and EndoAnchors (Medtronic, Heli-FX EndoAnchor System)). A second camera (Matrix Vision, mvBlueFox-IGC2bG; FOV: 33×33 mm; FPS=12.3) was placed on a fixed distance, perpendicular to the rail with the model, to film the measurement from outside of the silicon tube. The software also controlled the Arduino Mega 2560 board (Arduino), which controlled the motor (Dongbu Robot, Herkulex DRS 0402). The motor induced a longitudinal force on the endograft by pulling a plug that was connected to the endograft, with a wire. Furthermore, the Arduino was interfaced with a force sensor (Seneca, Z-SG) to determine the induced pulling force on the endograft. The force sensor was placed in between the motor and the plug and aligned with the model on a rail to provide a longitudinal pulling setup. A safety mechanism was built into the Arduino to stop the

measurement (e.g. pulling the endograft) automatically when too much force decay occurred. All the components of the measurement setup were calibrated and validated before the measurements were performed.

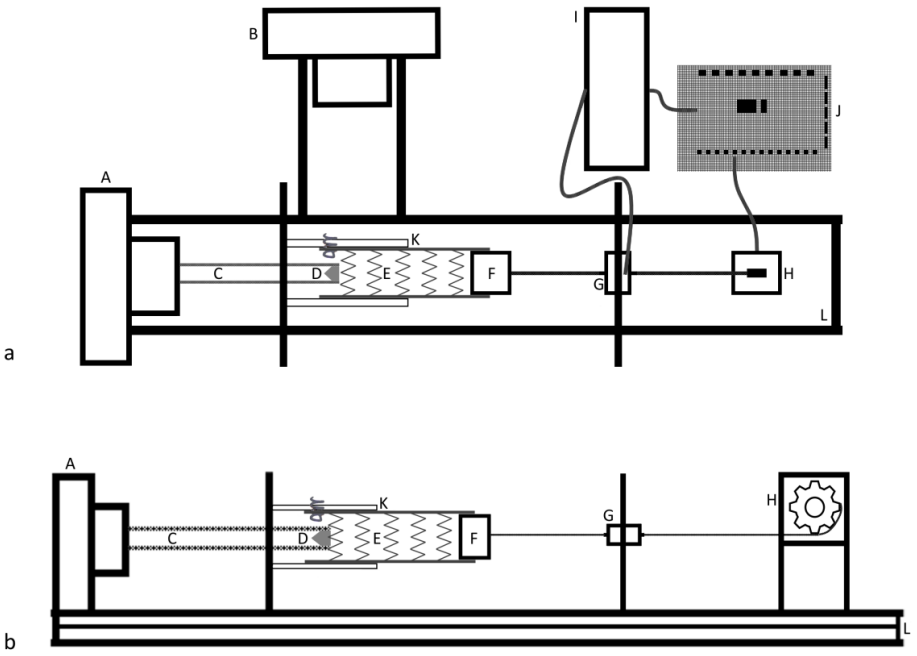

Figure 17. Schematic overview of measurement setup with a) the top view and b) the lateral view. The setup contains camera 1 (A), camera 2 (B), lens holder (C), mirror cone (D), endograft (E), pulling plug (F), force sensor (G), motor (H), force sensor converter (I), Arduino Mega 2560 (J), the silicon tube (K) and a rails (L) to mount all the components.

4.3.3 Force measurement

First, the endograft was placed in the measurement setup without EndoAnchors to perform a baseline measurement. A set of five measurements was performed to determine the force necessary to migrate the endograft and the variability between the measurements. This baseline measurement was used to determine the relative difference of the effect of EndoAnchor deployment versus the effect of no EndoAnchor deployment.

Based on thorough clinical evaluation of a previous patient cohort[22], four configurations (i.e. circumferential, 120 degrees of the circumference, deployment opposite to each other and a stack of EndoAnchors on one side) were investigated

to determine the effect of these different EndoAnchor configurations on proximal endograft migration resistance (Figures 18-21).

1. Circumferential deployment

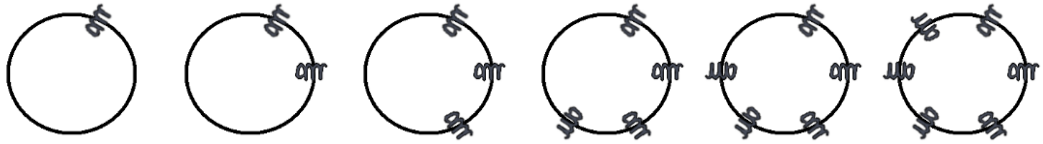

Figure 18. Protocol circumferential deployment. This configuration is build up to 6 EndoAnchors, where each step is tested

2. Deployment of EndoAnchors within 120 degrees on the circumferential vessel wall

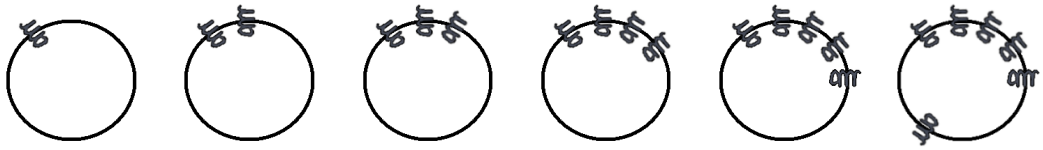

Figure 19. Protocol EndoAnchor deployment within 120 degrees. This configuration was build up to 6 EndoAnchors within approximately 120 degrees of the circumference

3. EndoAnchor placement in opposite position of each other

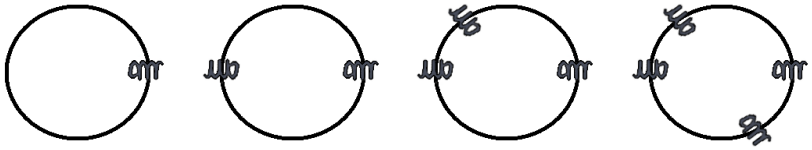

Figure 20. Protocol EndoAnchor deployment opposite to each other. This configuration was build up to 4 EndoAnchors

4. EndoAnchor deployment above each other

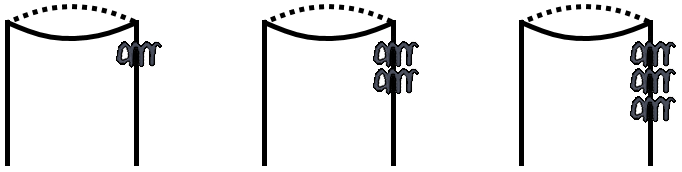

Figure 21. Protocol EndoAnchor deployment above each other. This configuration was built up to 3 EndoAnchors

The EndoAnchors were deployed by an experienced vascular surgeon under C-arm guidance to mimic the clinical setting. After deployment of each EndoAnchor, the model was placed back into the measurement setup and a set of five measurements were performed before the next EndoAnchor was deployed. The measurements consisted of longitudinally pulling the endograft with a constantly increasing pulling force, which was gradually increased in increments of 1 N until the endograft had visually displaced 3 mm, at which the measurement was terminated. A build-in safety of the software stopped the motor when a sudden decrease in force occurred (i.e. migration of the endograft) or if the force was 60 N. The force necessary to displace the endograft 3 mm was defined as the endograft migration force (EMF). If the applied pulling force also resulted in elongation of the hole(s) where the EndoAnchors were deployed into the silicon tube or damage to the endograft and/or EndoAnchors, a new set of measurements were performed with a new silicon tube, the next endograft ring and new EndoAnchors. The measurement protocol is attached in Appendix D.

4.3.4 Analysis

All measurements were performed five times, because early tests had shown consistent results during the same conditions. The data was assumed to be non-normally distributed, and hence data will be expressed as median [interquartile range (IQR)]. The videos were analysed to determine the effect of the pulling forces induced on the endograft, EndoAnchor and silicon tube.

4.4 Results

4.4.1 Camera view

Figure 22 explains the camera view of the mirror cone. Here, Figure 22a is a schematic view of the setup around the mirror cone, Figure 22b is the camera view of the mirror cone, and Figure 22c demonstrates the visualization of the endograft with EndoAnchor (*red arrow*) by the mirror cone. The orange and purple dots correspond to the locations of the mirror cone and the location within the camera image. The middle part of the image (*orange dot*) corresponds to the most proximal part of the mirror cone and thereby the endograft. The outer part of the image (*purple dots*) can be related to the most distal part of the mirror cone and thereby the endograft. Thus, the camera view ranges between the top and distal parts of the mirror cone (5 mm length). The orientation of the camera corresponds to the orientation of the cone, e.g. where the upper part of the image matches with

the upper part of the cone. If the endograft is migrating, this will start from the middle to the outer part in the camera image.

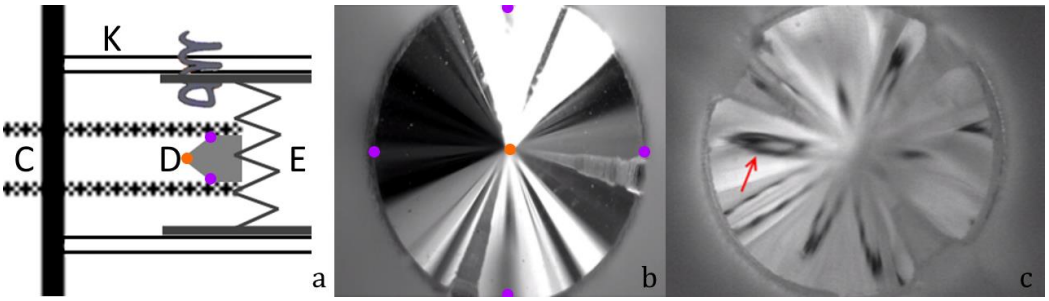

Figure 22. Representation of the mirror cone and camera view. a) A schematic depiction of camera 1 within the silicon tube (K) and endograft (E). The mirror cone (D) is fixed by the lens holder (C). The top of the mirror cone is represented by the orange dot, and the outer part (furthest point) with purple dots. b) View of the camera onto the mirror cone with the corresponding points (orange and purple dots). c) View of the camera onto the mirror cone within an endograft with deployed EndoAnchor (red arrow).

4.4.2 Configuration 1

Figure 23 illustrates the EndoAnchor deployment within the first configuration and the resulting EMFs of configuration 1 can be seen in table 4. The results of the measurements with one and two EndoAnchors appear to be the same, whereas adding EndoAnchors number three until six substantially increases the EMF. The large increase in difference in EMF between five and six EndoAnchors (i.e. from 300 degrees circumferential deployment to completely circumferential) can be noticed, where the EMF is respectively 26.7 and 42.2 N.

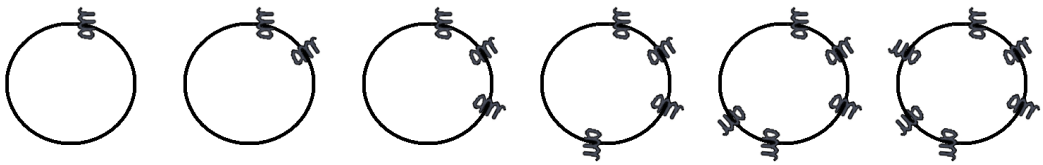

Figure 23. Actual EndoAnchor deployment of configuration 1

Analyzing the measurement videos, some remarkable things were noticed. As expected, every measurement showed the largest endograft migration at opposite side of where the EndoAnchors were deployed. Furthermore, slight migration also occurred at the location of the EndoAnchors, whereby some circumferential migration of the endograft was observed. When six EndoAnchors were deployed,

circumferential migration was barely seen. After the force was dropped, the endograft kicked back to its original position.

The outside camera revealed different stages of migration during increasing force on the endograft; first, migration of the endograft starts until the migration freedom surrounding the EndoAnchor is reached (Figure 24a), second, the EndoAnchor starts moving, resulting in changes in orientation of the EndoAnchor (Figure 24b), third, the endograft migrates to the lowest point of the EndoAnchor with regard to the pulling force (Figure 24c), if possible, and fourth, the silicon tube starts deforming. Moreover, struts were moving towards each other during several measurements (Figure 25).

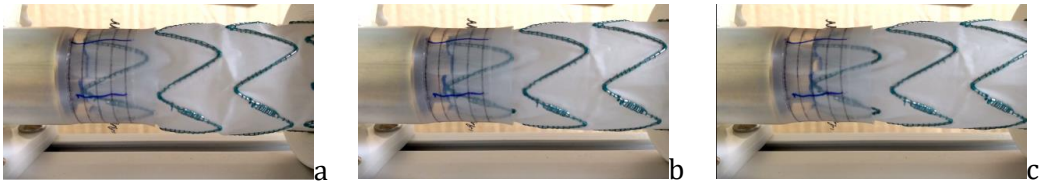

Figure 24. An overview of the different stages of migration a) stage 1 with migration with affecting any other component, b) stage 2 with changing position of the EndoAnchor and c) stage 3 and 4 with migration of the endograft and deformation of the silicon tube

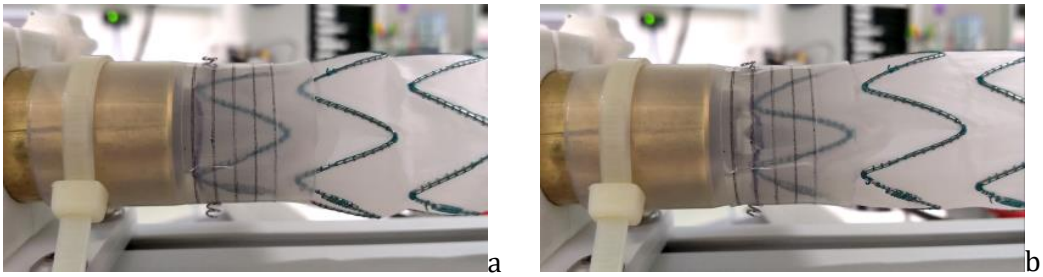

Figure 25. The illustration of endograft infolding during the measurements a) the starting point of the measurement and b) the struts are moved towards each other at the maximum applied force.

4.4.3 Configuration 2

For the second configuration, the results of one EndoAnchor were comparable to the previous results with one EndoAnchor. The endograft was positioned obliquely during measurement 1 with one EndoAnchor, which can explain the smaller EMF within table 5.

Table 4. Resulting EMF for configuration 1

Measurements	EMF (N) 1 EA	EMF (N) 2 EAs	EMF (N) 3 EAs	EMF (N) 4 EAs	EMF (N) 5 EAs	EMF (N) 6 EAs
1	6.8	8.1	10.6	22.3	26.7	59.0
2	7.6	7.6	10.1	22.5	27.0	46.8*
3	7.4	8.0	9.5	23.7	28.2	41.4*
4	7.7	8.1	10.8	25.0	26.3	42.4*
5	7.5	8.1	11.1	23.6	26.7	37.1*
Median [IQR]	7.5 [7.4-7.6]	8.1 [8.0-8.1]	10.6 [10.1-10.8]	23.6 [22.5-23.7]	26.7 [26.7-27.0]	42.4* [41.4-46.8]

* After measurement one, small fractures were seen in the endograft and the silicon showed small hole elongation, which could have influenced the subsequent measurements and thereby the median EMF of this number of EndoAnchors.

Table 5. Resulting EMF for configuration 2

Measurements	EMF (N) 1 EA	EMF (N) 2 EAs	EMF (N) 3 EAs	EMF (N) 4 EAs	EMF (N) 5 EAs	EMF (N) 6 EAs
1	6.5	8.9	9.7	12.4	18.0	28.0
2	8.3	8.4	10.5	11.7	17.5	30.6
3	8.3	9.3	9.8	12.4	17.6	29.7
4	8.2	9.2	9.7	12.2	17.0	28.9
5	8.2	9.4	10.2	11.6	17.2	29.0
Median [IQR]	8.2 [8.2-8.3]	9.2 [8.9-9.3]	9.8 [9.7-10.2]	12.2 [11.7-12.4]	17.5 [17.2-17.6]	29.0 [28.9-29.7]

Furthermore, one till three deployed EndoAnchors result in almost the same EMF, whereas four and five EndoAnchors create a larger difference. When the opposite EndoAnchor number six is deployed, the EMF increases substantially. Figure 26 shows the actual EndoAnchor deployment within this configuration.

Similar to the first configuration, migration occurred mostly at the opposite site than the EndoAnchor location, but some migration was also possible round the EndoAnchor. When all six EndoAnchors were deployed, most migration occurred between EndoAnchor number 6 and EndoAnchor 1 and 5, namely the largest parts of the endografts where no EndoAnchors were placed. Subsequently, this configuration also showed the endograft kickback when the force was dropped.

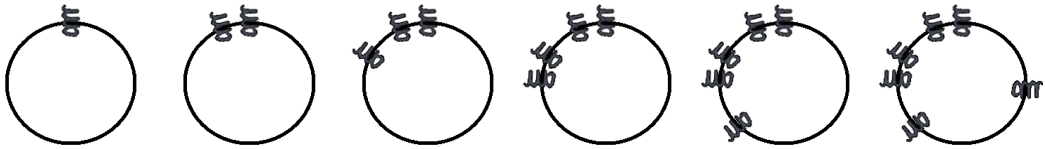

Figure 26. Actual EndoAnchor deployment of configuration 2

4.4.4 Configuration 3

Table 6 and Figure 27 respectively show the resulting EMF and deployment for configuration 3. Each EndoAnchor has a considerable impact on the EMF, where substantial differences between the numbers of deployed EndoAnchors can be seen.

Figure 27. Actual EndoAnchor deployment of configuration 3, with a final measurement of six circumferential deployed EndoAnchors. Here, a new EndoAnchor is deployed round the location of EndoAnchor number 2, which was dislodged from the endograft at the end of the measurements with four EndoAnchors

Table 6. Resulting EMF for configuration 3

Measurements	EMF (N) 1 EA	EMF (N) 2 EAs	EMF (N) 3 EAs	EMF (N) 4 EAs	EMF (N) 6 EAs
1	7.9	11.7	17.7	27.1	53.7
2	8.6	11.7	17.3	27.2	-
3	7.7	11.4	18.2	24.6*	-
4	8.0	11.1	18.0	24.1*	-
5	8.1	11.5	19.5	19.8*	-
Median [IQR]	8.0 [7.9-8.1]	11.5 [11.4-11.7]	18.0 [17.7-18.2]	24.6* [24.1-27.1]	

* After measurement two, the endograft fabric dislodged from one EndoAnchors started, where it was dislodged completely from the EndoAnchor during measurement number 5. This could have influenced the resulting EMF of measurement 3 till 5 and thereby the median EMF of this number of EndoAnchors.

Table 7. Resulting EMF for configuration 4

Measurements	EMF (N) 2 EAs	EMF (N) 3 EAs	EMF (N) 6 EAs
1	8.1	7.8	9.5
2	7.7	7.7	9.8
3	8.3	7.7	9.3
4	8.3	7.5	10.1
5	8.0	7.6	9.6
Median [IQR]	8.1 [8.0-8.3]	7.7 [7.6-7.7]	9.6 [9.5-9.8]

As would be expected, larger migration was observed at the location of folds of the endograft fabric (due to the oversizing). Furthermore, measurements with three EndoAnchors showed enlargement of the endograft folds. At the end of measurement 2 with six EndoAnchors, one EndoAnchor disconnected from the endograft. This EndoAnchor was positioned close to the proximal end of the endograft. Afterwards, the configuration was completed up to six EndoAnchors to create a circumferentially deployment.

When a second EndoAnchor was deployed opposite to the first one, migration was seen clearly in the regions between the EndoAnchors. The clear migration difference around the EndoAnchor and between the EndoAnchors can be seen in Figure 28b, where the EndoAnchors are highlighted with the red arrows.

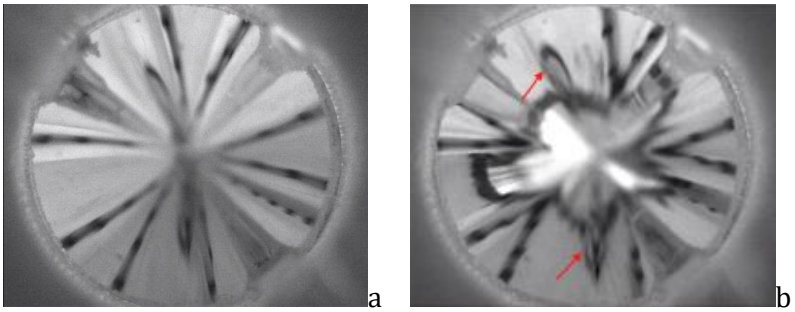

Figure 28. Endograft migration within configuration 3; a) the starting point of the measurement and b) the migration at the maximum applied force with migration of the endograft in between the EndoAnchors, where the migration can be identified with the proximal border of the endograft (thick black line) and where the EndoAnchors are highlighted with the red arrows

4.4.5 Configuration 4

Configuration 4 can be seen in Figure 29 and table 7 shows the resulting EMFs. Two and three EndoAnchors below each other resulted in nearly the same EMF and the second line of EndoAnchors induces a slightly higher EMF.

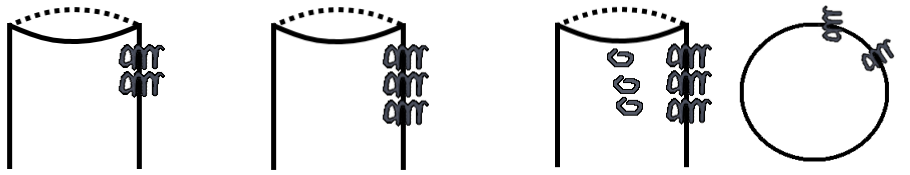

Figure 29. Actual EndoAnchor deployment of configuration 4, where the visualization of the measurement with six EndoAnchor also contains a top view (besides the lateral view) to illustrate the space between the two lines of EndoAnchors.

The videos of the measurements with two and three EndoAnchors below each other were nearly similar regarding the migration pattern of the endograft. Migration around the EndoAnchors was less than the other parts of the endograft. When the second line of EndoAnchors was placed, endograft migration mostly occurred at the opposite site of the EndoAnchors (Figure 30).

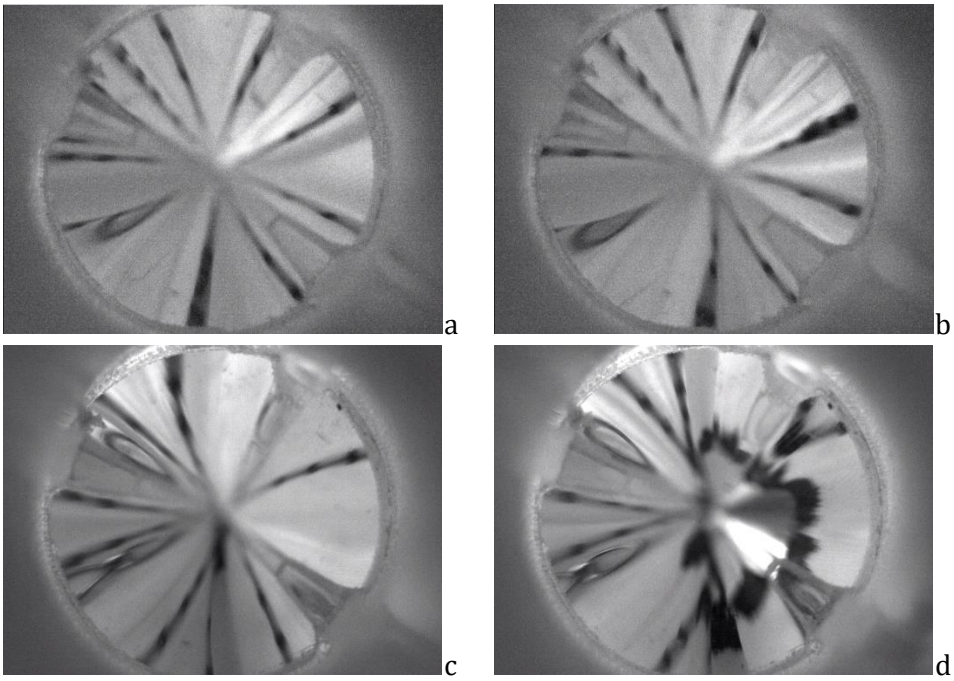

Figure 30. Illustration of the endograft migration when (a, b) two EndoAnchors are deployed within configuration 1 and (c, d) two lines of EndoAnchors are deployed within configuration 4

4.5 Discussion

This is the first manuscript to analyse the effect of different clinical EndoAnchor configurations on proximal endograft migration resistance in an *in-vitro* setup. The results showed that the endograft is prone to migration in the regions where no EndoAnchors had been deployed. Furthermore, the results demonstrated that the added value of EndoAnchor deployment to prevent endograft migration starts when a region of approximately 100-120 degrees of the endograft is covered with EndoAnchors according to the results of configuration 1 and 2.

Some interesting differences between the configurations were observed. First, the actual EndoAnchor deployment is slightly different from the EndoAnchor

configuration planned in the method. However, this is a good reflection of EndoAnchor deployment within clinical use. Another observation is the outcome of one deployed EndoAnchor which results in almost the same EMF within three different configurations. When EndoAnchors were added to the configurations, overall the EMF increases, but this depends greatly on the EndoAnchor position. The second EndoAnchor within configuration 3 increases the EMF with 3.5 N, whereas the second EndoAnchor in configuration 1 and 2 resulted in an increase in EMF of approximately 1 N. This difference highlights the importance of adequate distribution along the circumference. Furthermore, five EndoAnchors in approximately the same circumferential area in configuration 2 result in a higher EMF compared to three EndoAnchors spread out over a similar area in configuration 1. Thus, more EndoAnchors in a similar area can increase the EMF, but this is limited by the number of EndoAnchors delivered with the guide and applier. Additionally, the amount of migration between EndoAnchors is dependent of space between them. Furthermore, multiple EndoAnchors below each other also results in a bigger migration resistance on that part compared to only one row. The resulting EMF is not very different from one row, but less migration at the part of the EndoAnchors suggest that this configuration can be a good addition to treating gutters, chimneys and/or endoleaks.

The biggest difference between this study and other studies that determine fixation strengths of endografts (with EndoAnchors) is the resulting EMF. This can be explained by the difference in measurements, such as different materials than silicon, differences in definition for migration displacement (20 mm instead of 3 mm in this study), different lengths of sealing zone, and different pulling techniques.[20,33–36] This study focuses on the relative effect of EndoAnchors on endograft migration instead of the absolute effect. Thus, 3 mm displacement was sufficient to observe the location of endograft migration and to determine the relative migration resistance of the endograft. The increase in EMF of adding EndoAnchor number six to the circumferential configuration is noteworthy. This might suggest a relationship between the distance between EndoAnchors and the sensitivity to endograft migration in that region. This was also seen in the difference between five EndoAnchors in the circumferential configuration and configuration 2; five EndoAnchors deployed almost circumferentially resulted in a greater EMF than five EndoAnchors deployed within approximately 120 degrees of the endograft circumference. It also seemed that the migration resistance was bigger, when EndoAnchors were deployed more proximal to the endograft fabric

edge. Another intriguing outcome was the effect of deploying EndoAnchors below each other. Only one EndoAnchor may migrate slightly, whereas multiple EndoAnchors below each other demonstrated less migration around the EndoAnchors. This might suggest that the influence of deploying more than one row of EndoAnchors could counter the sensitivity of endograft migration and thereby increase the migration resistance at that part.

During the measurements and EndoAnchor deployment, the behaviour of EndoAnchors was observed. When force was applied on the endograft, longitudinal movement of the EndoAnchor and slight rotation of the EndoAnchor were seen. During the first measurement of a set of measurements, some EndoAnchors pretended to spin. Thereafter, the final position after spinning was the starting point for the next measurements. The clinical study of Van Noort et al.[31] described a large deviation between the longitudinal angles measured on CT scans of patients with EndoAnchor implants. This deviation can be explained by the ease in movement of the EndoAnchors when experiencing force during the measurements of this study. In addition, the measurements revealed that the first 1.5 mm migration occurred around 5 N and the other 1.5 mm migration variated with the amount and configuration of EndoAnchors. According to Molony et al.[21], this 5 N is comparable to clinical forces in the aortic vessel. The resulting EMFs of the measurement cannot be related to a clinical situation, but it does show the relative effect of the EndoAnchor movement when force is applied.

According to the IFU of EndoAnchors, four EndoAnchors should have been sufficient for the silicon diameter we used. However, we were interested in the relative effect of EndoAnchor configurations. Thorough analysis of follow-up data of patients treated with EndoAnchors identified several distribution patterns, which resulted in the decision to use six EndoAnchors to mimic these patterns at the same time.

An interesting observation was that the deployment of an EndoAnchor can result in displacement of the endograft, which can result in a smaller sealing zone than originally intended. Because of the deployment of the first EndoAnchor, the fabric in configuration 2 twisted and the endograft sealing zone decreased from 20 mm to 19 mm. The results demonstrated that 1 mm difference in sealing zone did not make a difference in resulting EMF. However, if deployment of more EndoAnchors also cause this displacement it may influence the EMF. Although, if the addition of

these EndoAnchors result in a circumferential configuration, influence on the EMF may be encountered. Moreover, EndoAnchor deployment within a fold resulted in penetration of double fabric, whereby a smaller penetration depth was observed. This observation can also be an explanation for smaller penetration depths of EndoAnchors found in recent clinical studies.[22,28,31] In addition, the struts also moved towards each other during the measurements. This could have resulted in enlargement of the folds during the measurement, what could influence migration analysis with the inner camera. Furthermore, the amount of oversizing is also expected to influence the EMF. During the validation of the setup, some measurements were performed with a 25 mm diameter silicon material, which created 20% oversizing and a smaller resistance to the endograft displacement. This silicon material demonstrated lower EMF values than the current used silicon material, respectively 7.7 N and 8.2 N with one deployed EndoAnchor.

Taking these study results into account, EndoAnchors should be deployed depending on the patient's anatomy and clinical situation. This study did not focus on EndoAnchor deployment within challenging aortic neck. However, the ideal EndoAnchor configuration for critical deployment should be determined for every situation. For example, a short neck might best be treated with two rows of six circumferential deployed EndoAnchors to prevent any migration. An angulated neck could benefit from more deployed EndoAnchors at the part where the endograft is more prone to migration than at the opposite part. However, circumferential deployment is still preferred.

There are some limitations to this study. The EMFs were determined by visual inspection, thereby inducing a human bias. Moreover, one Valiant endograft was used for this study; for every measurement one row of struts was used, after which this row was removed and the next row of struts was used for the next configuration. The results showed that the endograft seemed to be disentangled a little bit at some points, which seemed to become more during the measurements. This could have resulted in some structural damages in the fabric, what could have influenced the anchoring properties of the EndoAnchor with the endograft. Ideally, a new endograft would have been used for every configuration.

The measurements were performed horizontally with a constantly increasing pulling force, while one could argue to perform the measurements vertically with a pulsatile increasing pulling force to mimic the clinical situation more. Furthermore,

silicon material was chosen to simulate the aortic wall, while also animal material could have been chosen to have more similar characteristics to the aortic wall. Also, EndoAnchors are not always successfully deployed[22,28], but the effect of half deployed EndoAnchors on the sensitivity of endograft migration has yet to be investigated. However, the current study investigated the relative effect of EndoAnchor configurations on the proximal endograft migration, for which this measurement setup and protocol was sufficient.

4.6 Conclusion

This study demonstrates the migration behaviour of the endograft within different EndoAnchor configurations. If there is no circumferential deployment of EndoAnchors, the endograft remains relative sensitive to migration. Furthermore, this study showed that the distance between EndoAnchors has an influence on the migration resistance. In addition, the deployment of a second (or third) row of EndoAnchors also demonstrated to increase the migration resistance of the endograft. The ideal EndoAnchor configuration should be determined for every patient's anatomy.

5. General discussion and future perspectives

The aim of this thesis was to investigate the effect of EndoAnchor positioning and penetration depth with the focus on proximal fixation on the occurrence of endoleaks and migration. Clinical as well as technical research was performed, which demonstrated both good and promising results regarding the effect of EndoAnchor deployment.

The follow-up study showed a good sustainability of individual EndoAnchors at a median follow-up of 13 months. Only five of the 187 initially good penetrating EndoAnchors changed in penetration depth, but without clinical sequalae. This study highlighted the importance of the position and penetration of EndoAnchors, where 48% of all initially implanted EndoAnchors were maldeployed due to deployment beyond recommended use. This study emphasized the importance of positioning the EndoAnchor as proximal as possible in the endograft fabric. In this way, change in EndoAnchor position can be prevented. The *in-vitro* study supported the importance of EndoAnchor positioning. When EndoAnchors were deployed more distally, the endograft showed a smaller migration resistance. Furthermore, EndoAnchors demonstrated to be susceptible to some movement, even within the smaller force ranges. This could explain the large deviation in longitudinal angles in the follow-up study. Moreover, the *in-vitro* study indicated the influence of space between EndoAnchors on the sensitivity of endograft migration.

There are some limitations of the current studies. First, the population of the follow-up study was small and confined with a median follow-up time of 13 months. Ideally, a more general overview of the EndoAnchor's sustainability should be obtained to determine the durability and stability of the EndoAnchors in general. Second, the amount of performed measurements of the *in-vitro* study is small. Third, the *in-vitro* study investigated only one type of endograft, while more types of endografts are used in daily practice. Finally, the *in-vitro* study focused on the migration behaviour in a straight tube. However, patients often have challenging aortic necks, for example conical or angulated necks, which can have a big influence on the migration behaviour of the endograft.

Future research could focus on obtaining more clinical information about the EndoAnchor functioning in the human body to determine the EndoAnchor behaviour when experiencing a pulling force by the blood pressure. Dynamic CT scans could provide this information. However, the patient population suffering

from endograft migration after EndoAnchor deployment is small. Furthermore, it is interesting to investigate if the determined EndoAnchor behaviour in the *in-vitro* study is comparable within other types of endografts. Moreover, it is of added value to understand the effect of challenging aortic necks on the sensitivity to endograft migration, when EndoAnchors are deployed.

Overall, this thesis demonstrated the importance of the effect of positioning and penetration of EndoAnchors on the occurrence of endoleaks and migration. When EndoAnchors are initially good deployed, the sustainability of the EndoAnchors is excellent. However, the positioning and deployment within recommended use is important. Furthermore, the *in-vitro* study demonstrated that use of EndoAnchors for preventing endograft migration will only be useful when they are deployed circumferential. Future research should focus on the effect of EndoAnchors on migration behaviour in different endografts and environments which mimic the challenging necks patients could have.

6. Acknowledgement

During my thesis, many people helped me in various ways. I would like to express my gratitude to them for their kind support.

First, I would like to thank Jean-Paul de Vries for the opportunity to perform research at the vascular department at the St. Antonius Hospital, Nieuwegein. You offered me the chance to perform my research partially at Syntactx in New York, which was a valuable experience. In addition, I appreciate all the time and effort you have put in helping me with my research and experiments. Your clinical perspective and comments on the research were very useful. Furthermore, I would like to thank Kees Slump for all the technical feedback. You have taught me to look closer and more critical at my work to make it more accurate. I would also like to thank Rian Haarman for all the good talks and for helping me learning more about myself and to develop a better (professional) version of myself. Additionaly, I would like to thank Seline Goudeketting for always being there when I had questions and for taking time to provide me with valuable comments on this thesis. I also appreciate all the trips to Enschede and all the help with the measurements. Subsequently, I would also like to thank Kim van Noort for all the help and support during my research and experiments.

Second, I would like to thank dr. Kenneth Ouriel and Joy Bracker for taking care of me while being in New York. You made me feel at home right away in the Big Apple. I would also like to thank Gerben te Riet o.g. Scholten and Henny Kuipers for all the help and support with my measurement setup.

Third, I would like to thank the whole vascular research department. Without you my days would not have been as much fun. I appreciate all the valuable input given during the coffee breaks and above all the great work environment: Richte, Stefan, Simon, Elyse, Leontien and Annemiek.

Finally, my special thanks goes to my family and my close friends for their unconditional support during my study and especially during this last year. You always showed interest and took the time to hear me out.

7. Bibliography

1. Gianfagna F, Veronesi G, Bertù L, et al. Prevalence of abdominal aortic aneurysms and its relation with cardiovascular risk stratification: protocol of the Risk of Cardiovascular diseases and abdominal aortic Aneurysm in Varese (RoCAV) population based study. *BMC Cardiovasc Disord*. 2016;16(243):1-8.
2. Sun Z. Abdominal aortic aneurysm: Treatment options, image visualizations and follow-up procedures. *J Geriatr Cardiol*. 2012:49-60.
3. Ailawadi G, Eliason JL, Upchurch GR, Arbor A. Current concepts in the pathogenesis of abdominal aortic aneurysm. *J Vasc Surg*. 2003;38(03):584-588.
4. Abdul-hussien H, Hanemaaijer R, Kleemann R. The pathophysiology of abdominal aortic aneurysm growth: Corresponding and discordant inflammatory and proteolytic processes in abdominal aortic and popliteal artery aneurysms. *J Vasc Surg*. 2010;51(6):1479-1487.
5. Wanhainen A, Bergqvist D, Boman K. Risk factors associated with abdominal aortic aneurysm: A population-based study with historical and current data. *J Vasc Surg*. 2005;41(3):390-396.
6. Greenhalgh RM, Powell JT. Endovascular Repair of Abdominal Aortic Aneurysm. *N Engl J Med*. 2008;358(5):494-501.
7. Aggarwal S, Qamar A, Sharma V, Sharma A. Abdominal aortic aneurysm: A comprehensive review. *Exp Clin Cardiol*. 2011;16(1):11-15.
8. Mohan IV, Laheij RJF, Harris PL. Risk Factors for Endoleak and the Evidence for Stent-graft Oversizing in Patients Undergoing Endovascular Aneurysm Repair. *Eur J Vasc Endovasc Surg*. 2001;21:344-349.
9. Sternbergh WC, Money SR, Greenberg RK, Chuter AM, Orleans N, Francisco S. Influence of endograft oversizing on device migration, endoleak, aneurysm shrinkage, and aortic neck dilation: Results from the Zenith multicenter trial. *J Vasc Surg*. 2004;39(1):20-26.
10. Chaikof EL, Blankensteijn JD, Harris PL, et al. Reporting standards for endovascular aortic aneurysm repair. *J Vasc Surg*. 2002;35(5):1048-1060.
11. Gandhi RT, Katzen BT. Treating a Type Ia Endoleak Using EndoAnchors. *Endovasc today*. 2012;(maart):23-26.
12. Vries JPPM de, Pavoordt HDWM van de, Jordan WD. Rationale of EndoAnchors in abdominal aortic aneurysms with short or angulated necks. *J Cardiovasc Surg*. 2013;54(5):1-5.
13. Bail DHL, Walker T, Giehl J. Vascular Endostapling Systems for Vascular Endografts (T)EVAR — Systematic Review — Current State. *Vasc Endovascular Surg*. 2013;47(4):261-266.
14. Avci M, Vos J, Kolvenback R, et al. The use of endoanchors in repair EVAR cases to improve proximal endograft fixation. *J Cardiovasc Surg (Torino)*. 2012;53(4):419-426.
15. Liffman K, Lawrence-Brown MM, Semmens JB, Bui A, Rudman M, Hartley DE. Analytical modeling and numerical simulation of forces in an endoluminal graft. *J Endovasc Ther*. 2001;8(4):358-371.
16. Rodway AD, Powell JT, Brown LC, Greenhalgh RM. Do Abdominal Aortic Aneurysm Necks Increase in Size Faster after Endovascular than Open Repair? *Eur J Vasc Endovasc Surg*. 2008;35(6):685-693.

17. Oberhuber A, Buecken M, Hoffmann M, Orend KH, Mhling BM. Comparison of aortic neck dilatation after open and endovascular repair of abdominal aortic aneurysm. *J Vasc Surg*. 2012;55(4):929-934.
18. Tassiopoulos AK, Monastiriotis S, Jordan WD, Muhs BE, Ouriel K, Vries JP de. Predictors of early aortic neck dilatation after endovascular aneurysm repair with EndoAnchors. *J Vasc Surg*. 2017;66(1):45-52.
19. Gomero-Cure W, Mehta M, Fairman RM, Henretta JP, Glickman MH, Deaton DH. RR18. Helical Endostaple Fixation Blunts Aortic Neck Dilatation after Endovascular Aortic Aneurysm Repair. *J Vasc Surg*. 2012;55(6).
20. Melas N, Perdikides T, Saratzis A, Saratzis N, Kiskinis D, Deaton DH. Helical EndoStaples enhance endograft fixation in an experimental model using human cadaveric aortas. *J Vasc Surg*. 2012;55(6):1726-1733.
21. Molony DS, Kavanagh EG, Madhavan P, Walsh MT, McGloughlin TM. A computational study of the magnitude and direction of migration forces in patient-specific abdominal aortic aneurysm stent-grafts. *Eur J Vasc Endovasc Surg*. 2010;40(3):332-339.
22. Goudeketting SR, Noort K Van, Ouriel K, et al. [Accepted] Influence of aortic neck characteristics on successful aortic wall penetration of EndoAnchors in therapeutic use during endovascular aneurysm repair. *J Vasc Surg*.
23. Jordan WD, Vries JPM De, Ouriel K, et al. Midterm Outcome of EndoAnchors for the Prevention of Endoleak and Stent-Graft Migration in Patients With Challenging Proximal Aortic Neck Anatomy. *J Endovasc Ther*. 2015;22(2):163-170.
24. Galinanes EL, Hernandez E, Krajcer Z. Preliminary Results of Adjunctive Use of EndoAnchors in the Treatment of Short Neck and Pararenal Abdominal Aortic Aneurysms. *Catheter Cardiovasc Interv*. 2016;87:154-159.
25. Vries JPM de, Ouriel K, Mehta M, Varnagy D. Analysis of EndoAnchors for endovascular aneurysm repair by indications for use. *J Vasc Surg*. 2014;60(6):1460-1468.
26. Jordan WD, Mehta M, Ouriel K, et al. One-year results of the ANCHOR trial of EndoAnchors for the prevention and treatment of aortic neck complications after endovascular aneurysm repair. *Vascular*. 2016;24(2):177-186.
27. Vries JPPM, Jordan WD. Improved fixation of abdominal and thoracic endografts with use of EndoAnchors to overome sealing issues. *Gefässchirurgie*. 2014;19(3):212-219.
28. Goudeketting SR, Noort K van, Vermeulen JJM, et al. [Submitted] Analysis of the position of EndoAnchors in therapeutic use during EVAR. 2017.
29. Muhs BE, Jordan W, Ouriel K, Rajaee S, Vries JP de. Matched cohort comparison of endovascular abdominal aortic aneurysm repair with and without EndoAnchors. *J Vasc Surg*. 2018;67(6):1699-1707.
30. Medtronic. *Aptus Heli-FX EndoAnchor System - Instruction For Use.*; 2001.
31. Noort K van, Vermeulen JJM, Goudeketting SR, Ouriel K, Slump CH, Vries JPPM de. [Submitted] Sustainability of individual EndoAnchor implants in therapeutic use during endovascular aortic aneurysm repair. 2018.
32. Han K, Ishmaku A, Xin Y, et al. Mechanical properties of MP35N as a reinforcement material for pulsed magnets. *IEEE Trans Appl Supercond*. 2002;12(1):1244-1247.
33. Deaton DH. Improving Proximal Fixation and Seal with the HeliFx Aortic EndoAnchor. *Semin Vasc Surg*. 2012;25(4):187-192.

34. Andrews SM, Anson AW, Greenhalgh RM, Nott DM. In vitro evaluation of endovascular stents to assess suitability for endovascular graft fixation. *Eur J Vasc Endovasc Surg*. 1995;9(4):403-407.
35. Arko FR, Heikkinen M, Lee ES, Bass A, Alsac JM, Zarins CK. Iliac fixation length and resistance to in-vivo stent-graft displacement. *J Vasc Surg*. 2005;41(4):664-671.
36. Bosman WMPF, Steenhoven TJ v. d., Suárez DR, Hinnen JW, Valstar ER, Hamming JF. The Proximal Fixation Strength of Modern EVAR Grafts in a Short Aneurysm Neck. An In Vitro Study. *Eur J Vasc Endovasc Surg*. 2010;39(2):187-192.
37. Donselaar EJ, Van Der Vijver-Coppen RJ, Van Den Ham LH, Lardenoye JWHP, Reijnen MMPJ. EndoAnchors to resolve persistent type Ia endoleak secondary to proximal cuff with parallel graft placement. *J Endovasc Ther*. 2016;23(1):225-228.
38. Kasprzak P, Pfister K, Janotta M, Kopp R. EndoAnchor Placement in Thoracic and Thoracoabdominal Stent-Grafts to Repair Complications of Nonalignment. *J Endovasc Ther*. 2013;20(4):471-480.

8. Appendices

Appendix A: Technical background angle measurement

The orientation of EndoAnchor penetration is defined by two angles; the orthogonal and the longitudinal angle. The orthogonal angle (Figure 31A) is measured with the 3Mensio angle tool. Because there was no tool to measure the longitudinal angle, this angle was calculated in a slightly different way using 3Mensio marker coordinates and MATLAB. First, markers were placed on the extremities of the EndoAnchor (*purple dots*, ***iea [inner EndoAnchor]*** and ***oea [outer EndoAnchor],*** Figure 31B). Parallel to the EndoAnchor extremities, markers were placed on the aortic wall (*orange dots*, ***ivw [inner vascular wall]*** and ***ovw [outer vascular wall]***, Figure 31B). In this way, the coordinates of these markers in space could be obtained. Directional vectors (*black arrows,* Figure 31B) were calculated for the EndoAnchor and the aortic wall (respectively, Equations 1 and 2).

$$\boldsymbol{dU} = ((oea(x) - iea(x)), (oea(y) - iea(y)), (oea(z) - iea(z))) \quad (1)$$

$$\boldsymbol{dV} = ((ovw(x) - ivw(x)), (ovw(y) - ivw(y)), (ovw(z) - ivw(z))) \quad (2)$$

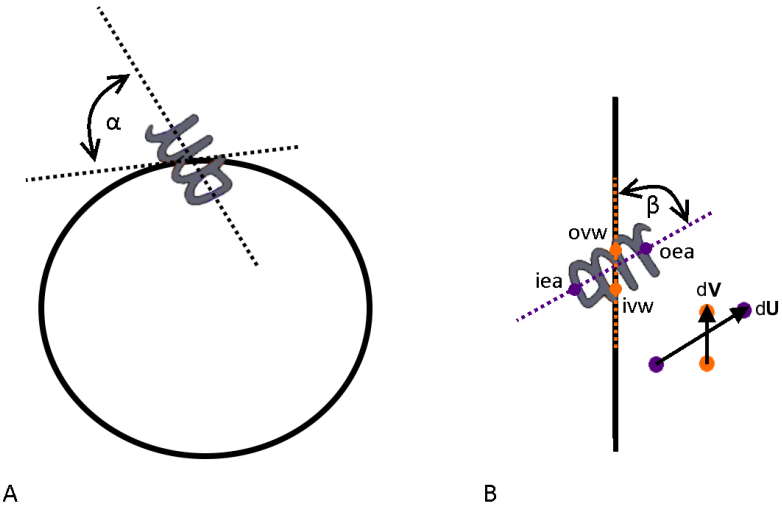

Figure 31. Schematic illustration of the definition of the orthogonal and longitudinal angle of the EndoAnchor with the aortic wall. A) The orthogonal angle (α) of the EndoAnchor with the interface plane of the aortic wall. B) The longitudinal angle (β) of the EndoAnchor with the aortic wall is calculated between the directional vector of the aortic wall (vector between *orange dots*) and the EndoAnchor (vector between the *purple dots*).

Subsequently, a rotation matrix is calculated to orientate the directional vector of the vessel wall (***dV***) with the z-axis (Figure 32C). This rotation matrix is multiplied with the directional vector of the EndoAnchor (***dU***) to obtain the same orientation to calculate the correct longitudinal angle for every EndoAnchor. The defined orientation for the longitudinal angle can be seen in Figure 32.

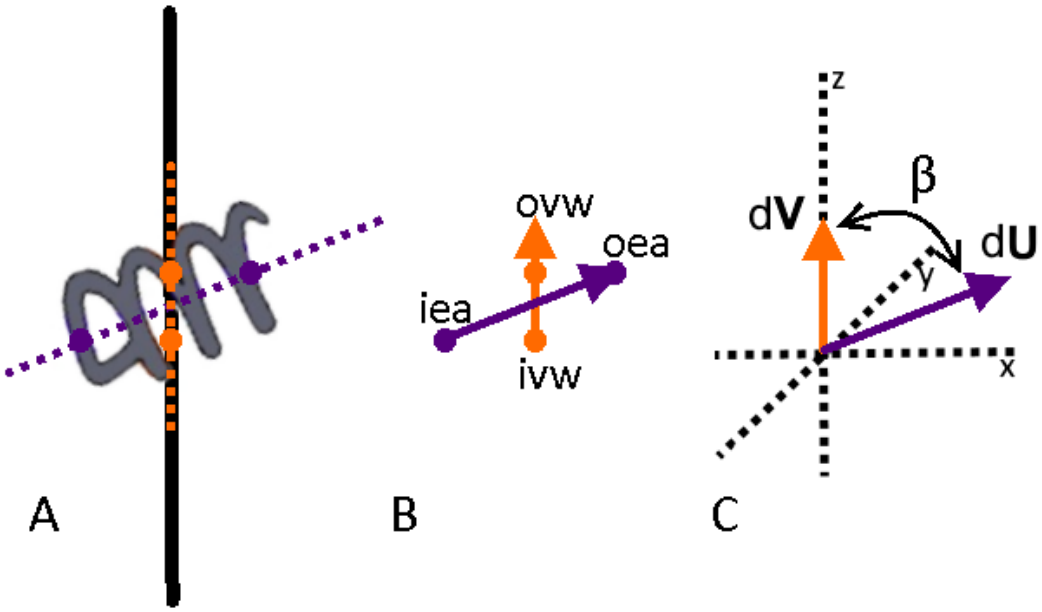

Figure 32. Schematic depiction and definition of the longitudinal angle (β) orientation between the EndoAnchor and the aortic wall. A) The EndoAnchor (*purple line and dots*) orientation regarding the aortic wall (*orange line and dots*). B) The directional vector of the EndoAnchor (*purple arrow*) and the aortic wall (*orange arrow*). C) The directional vectors are placed in the origin with the directional vector of the vessel wall parallel to the z-axis and the longitudinal angle (β) is defined.

The final step is to calculate the angle between the two directional vectors ***dU*** (U_1, U_2, U_3) and ***dV***. First, the Euclidean length of the EndoAnchor is determined (Equation 3). This length is needed to calculate the longitudinal angle (Equation 4).

$$Pxy_{ea} = \|d\boldsymbol{U}\| = \sqrt{{U_1}^2 + {U_2}^2 + {U_3}^2} \quad (3)$$

$$Angle = \operatorname{atan}\left(\frac{U_3}{Pxy_{ea}}\right) \times \frac{180}{\pi} \quad (4)$$

Appendix B: Materials and requirements

Components measurement setup

- Camera (Type: mvBlueFox-IGC202bG)
- Force sensor (Type: Seneca Z-SG)
- Herkulex servo module (Type: DRS 0402)
- Arduino Mega 2560
- Silicon tube (24 mm inner diameter)
- Valiant thoracic stent graft (30 mm diameter)
- EndoAnchors
- Parts to fixate different components
- Connecting cables
- Pc with MATLAB

Requirements

1. Camera is functioning

Why: Camera needs to record what happens to the EndoAnchors and the endograft during the measurements.

Achieved:
- When the camera sees the endograft as well as the EndoAnchors
- When the camera records from the start of pulling the endograft till migration or damage to EndoAnchor, graft or silicon tube occurs
- When the camera has a 360-degree view
- When the camera does not move during the measurements and thereby the focal point in order to see the measurement clearly

2. Force sensor needs to show reliable results

Why: Force sensor must give feedback about the executed force during the measurement.

Achieved:
- When the pc obtains the data from the force sensor
- When the force sensor is calibrated for certain weights and force changes

3. The Herkulex servo module is functioning

Why: The Herkulex servo module must induce the pulling force on the stent

Achieved:
- When the Herkulex servo module can be controlled to start and stop moving

- When the Herkulex servo module is connected to the force sensor and the endograft to create a pulling force of maximum 100 N on the stent

4. Arduino is functioning

Why: The Arduino needs to control the measurement setup by driving every component when necessary during the measurement.

Achieved:
- When the Arduino can start and stop the motor
- When the Arduino can obtain data from the force sensor
- When the boundary conditions within the Arduino function to stop the motor to guarantee safety:
    - When the induced force exceeds 60 N.
    - When the induced force decreases with an amount of 2 N.

5. Silicon tube needs to simulate the aortic wall and needs to resist forces which are applied on the tube

Why: The silicon tube needs to meet some conditions to create a measurement setup which simulate the aortic wall and resist forces when an endograft and EndoAnchors are placed in the abdominal aorta.

Achieved:
- When the silicon tube generates a 25% oversizing of the endograft
- When the silicon tube does not tear before endograft migration occurs
- When the silicon tube does not deform when it experiences a force of 100 N.

6. The fixation of the endograft must be comparable to the conditions of the endograft in the body

Why: The endograft needs to meet some conditions in order to investigate the correct variables, but also to create a measurement setup which can relate to the physiological conditions when an endograft and EndoAnchors are placed in the abdominal aorta.

Achieved:
- When the bare metal struts and barbs of the endograft have been removed
- When pulling forces can be induced on the endograft without causing damage to the endograft (i.e. with the plug).
- When the endograft is pulled in a straight line in order to induce forces on the endograft like in the human body

7. MATLAB should be functioning to control the measurement setup

Why: MATLAB must integrate different setup components to control the measurement setup.

Achieved: - When MATLAB can start, stop and record the video images
- When MATLAB can obtain data from the force sensor
- When MATLAB can start and stop the motor
- When MATLAB contains some boundary conditions to stop the motor to guarantee safety:
    - When the induced force exceeds 60 N.
    - When the induced force decreased with an amount of 2 N.
    - An emergency stop to terminate all components.

Appendix C: Test protocol

Test 1: Calibration of the force sensor

Setup: Attach certain weights to the force sensor.

To do: Test three different weights several times to make sure the force sensor is calibrated sufficiently. Additionally, a test is done where the force is built up.

Test:

- Functionalities software:
  - Calibration of the force sensor, including calibration of force changes
  - Arduino functionalities as described in requirements regarding the force sensor
  - MATLAB functionalities as described in requirements regarding the force sensor

Test 2: Calibration of the camera view of the cone

Setup: Place a calibration pattern within the silicon tube to see with the cone, which is seen with the camera.

To do: Start camera and determine the elongation of the image, which is seen with the camera.

Test:

- The camera view characteristics to determine the distances seen in the video images

Test 3: Testing the functionalities of the silicon tube

Setup: Attach the pulling mechanism to the tube and perform the measurement. In this way, there can be determined whether there is a correlation between the amount of force and stretching of the silicon tube. This can be done in three settings: marking a place on the tube with a dot, making a 5 mm incision in longitudinal direction and in orthogonal direction in the silicon tube.

To do: Build up the force till 60 N to see what happens and afterwards you keep increasing till 100 N to see whether something changes with the silicon tube.

Test:

- The characteristics of the silicon tube, when it experiences a certain amount of force

Test 4: Testing the functionalities of the measurement setup

Setup: Implement a dummy endograft in the measurement setup and pull the endograft. A needle can be inserted transversal through the silicon tube and the endograft to simulate the anchoring of an EndoAnchor.

To do: Test this setup until all functionalities and boundary conditions are determined.

Test:

- Functionalities software:
  - Camera functionalities as described in requirements
  - Herkulex servo module functionalities as described in requirements
  - Arduino functionalities as described in requirements
  - MATLAB functionalities as described in requirements
- Boundary conditions measurement setup to integrate in the software

Test 5: Determine if the EndoAnchors are reusable

Setup: Deploy EndoAnchor in measurement setup and perform the measurement several times. The measurement is terminated when migration of the endograft occurs. When the results show:

- no difference, measurements can be performed several times with the same EndoAnchor, which is already placed
- a difference, new EndoAnchors need to be placed every time we perform a measurement

To do: Perform this measurement approximately 50 times with one EndoAnchor to determine whether exposing the EndoAnchor to the same force several times alters the EndoAnchor's functioning. During the measurements, a maximum of 6 EndoAnchors are present within one configuration. Measurements are performed 5 times per EndoAnchor placement, which will result in approximately 30 measurements on one EndoAnchor after placement.

Test:

- Whether there is a significant difference between force necessary to cause endograft migration when an EndoAnchor is placed in the measurement setup for the first time and when the EndoAnchor already underwent a force several times.

Test 6: Testing functionalities of the measurement setup with the endograft

Setup: Place the endograft in the measurement setup and performing the measurement without EndoAnchors. The measurement is terminated when migration of the endograft occurs.

To do: The measurement is performed several times to validate the setup and the baseline measurement is performed at least 5 times to obtain a reliable result of the force that is necessary to cause migration of the endograft without EndoAnchors.

Test:

- Validation of the measurement setup:
  - Camera range and functionalities as described in requirements.
  - The pulling mechanism of the endograft
  - Herkulex servo module functionalities as described in requirements
  - Arduino functionalities as described in requirements
  - MATLAB functionalities as described in requirements
  - Silicon tube functionalities as described in requirements
  - Endograft functionalities as described in requirements
- Baseline measurement to determine the force necessary to cause migration of the endograft without EndoAnchors
- Evaluate if boundary conditions of test 4 are accurate for the real measurements with endograft

Appendix D: Measurement protocol

Research question

What is the effect of different EndoAnchor configurations on proximal endograft migration resistance when a constantly increasing force is applied?

Preparation

In order to get started, the EndoAnchor configurations are built up as shown in figure 33-36. Before the start of the measurement, the settings and functionalities of the system are tested once more. Then, the endograft and the appropriate number of EndoAnchors are placed at the preferred location. At last, the pulling mechanism is connected to the endograft to start the measurement.

Durability test of the EndoAnchors were previously performed and showed minor hole elongation at the location of the EndoAnchor. This occurred between the 300 and 400 million heart cycles. For these tests, endografts comparable to the Valiant thoracic stent graft (i.e. same graft material and construction) were used. These measurements were performed under severe test conditions (worst-case axial loading), but still no tearing of the fabric or pulling out of the EndoAnchor was observed. Therefore, it can be assumed that the endograft with the same deployed EndoAnchor(s) can experience force multiple times.[30]

Calibration

The calibration for these measurements are performed during the validation of the measurement setup. This means that the setup is calibrated once for all the measurements.

Measurements

Based on clinical knowledge of EndoAnchor positioning in patients, four configurations will be tested:

1. Circumferential deployment

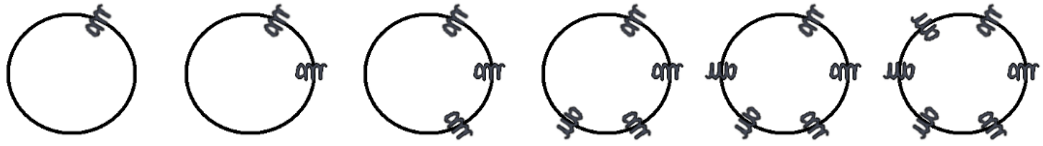

Figure 33. Protocol circumferential deployment. This configuration is build up to 6 EndoAnchors, where each step is tested

2. Deployment of EndoAnchors within 120 degrees on the circumferential vessel wall

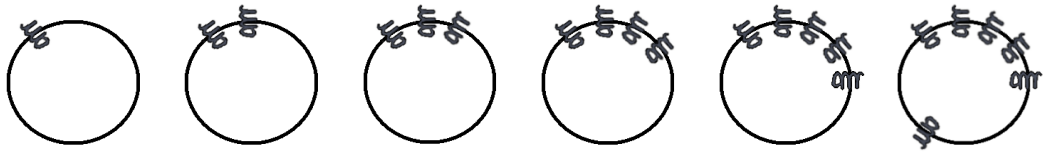

Figure 34. Protocol EndoAnchor deployment within 120 degrees. This configuration was build up to 6 EndoAnchors within approximately 120 degrees of the circumference

3. EndoAnchor placement in opposite position of each other

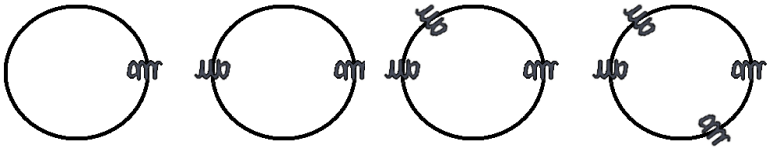

Figure 35. Protocol EndoAnchor deployment opposite to each other. This configuration was build up to 4 EndoAnchors

4. EndoAnchor deployment above each other

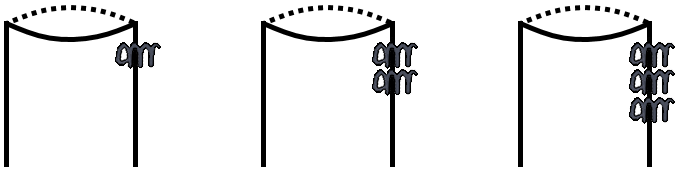

Figure 36. Result EndoAnchor deployment above each other. This configuration was built up to 3 EndoAnchors

Each configuration is tested. The measurement is terminated, when migration or damage to EndoAnchor, graft or silicon occurs. If none of the components is damaged, these measurements are repeated five times per EndoAnchor.

Analysis

After the measurements, the obtained data is analysed to see whether there is an effect of the EndoAnchor position on the endograft migration resistance. Non-normally distributed data is assumed. Therefore, the median [IQR] will be used to display the results. The different steps per configuration will be compared with each other to see whether there is a difference in adding EndoAnchors to the configuration. Also, the different configurations will be compared with each other

to determine whether the type of configuration influences the effect on endograft migration resistance. Furthermore, the videos are analysed to determine the effects of the forces which are induced on the endograft, EndoAnchor and silicon tube.

Hypothesis

The hypothesis on these measurements contain several components.

- Displacement of the endograft is expected to occur (primarily) on the endograft area without EndoAnchors.
- The force necessary to generate endograft migration will increase linear when deploying EndoAnchors next to each other. The linearity is expected to be influenced by the part of the vessel wall covered with EndoAnchors and by the number of EndoAnchors. We assume that the area over which EndoAnchors are deployed (circumferentially) is of greater importance than the number of EndoAnchors deployed.
- The expected force to generate 3 mm endograft migration are displayed in the tables below divided for each configuration and each added EndoAnchor. This hypotheses are based on the research of Melas et al. (2012)[20] and displayed in Table 8.

Table 8. Expected resulting EMF from all the test, divided per configuration (baseline, 1, 2, 3 and 4) and per EndoAnchor

Test	EMF (N)
Baseline	10
1.1	20
1.2	30
1.3	40
1.4	50
1.5	60
1.6	70

Test	EMF (N)
2.1	20
2.2	25
2.3	30
2.4	35
2.5	40
2.6	50

Test	EMF (N)
3.1	20
3.2	40
3.3	45
3.4	55

Test	EMF (N)
4.1	20
4.2	25
4.3	25